AN ABSTRACT OF THE THESIS OF

James Benjamin Phipps (Name) for the Doctor of Philosophy (Degree)

in Oceanography (Major) presented on September 5, 1973 (Date)

Title: SEDIMENTS AND TECTONICS OF THE GORDA-JUAN DE FUCA PLATE

Abstract approved: Redacted for Privacy

Cores taken from the ridge areas of the Gorda-Juan de Fuca plate have a sedimentation rate that is appropriate for the study of late Quaternary stratigraphy. An analysis of the clay and silt mineralogy of the cores using X-ray diffraction methods and by noting changes in the foraminiferan-radiolarian abundances in the cores were utilized in developing a stratigraphic sequence.

The clay fractions of these sediments consists of chlorite, illite and smectite. Cores taken from bathymetric highs contain, on the average, less smectite than do the turbidites from the adjacent lowlands. The low smectite content suggests eolian enrichment of these sediments since dusts collected from the nearby continent also have low smectite concentrations.

Changes in the relative abundances of radiolaria and foraminifera are used to put biostratigraphic constraints on the correlation of

mineralogical datums. Two changes in the foraminiferan-radiolarian ratios, marked by sharp increases in the abundance of radiolaria, occurred at 12,500 years B.P. and 83,000 years B.P. as dated by carbon-14 and sedimentation rate extrapolations, respectively. Such faunal changes serve as an independent check of correlations of the mineralogical datums.

In the 2 to 20 micron, silt fraction, quartz, chlorite, mica and feldspar are the predominant minerals. Intervals in which the relative abundance of quartz changes can be dated by carbon-14 and sedimentation rates, and related to late Quaternary climatic events. The quartz-rich zones are synchronous with periods of high insolation, high stands of sea-level, and to a lesser degree with the catastrophic floods of the Columbia River. The correlation with high solar radiation reflects quartz enrichment of the sediment due to an increased eolian contribution. The coincident high sea level stands effectively decreased the sedimentation rate of quartz-poor continental detritus that otherwise dilutes the eolian component. The periodic floods of the Columbia River, caused by the failure of ice dams, swept quartz-rich loess from eastern Washington down the river and injected into the marine environment. Such sediment also increased the quartz abundance in the quartz-rich zones on the ridges. Thus, the late Quaternary stratigraphy of the cores can be related to global late Quaternary climatic variations as well as to

events recorded on the adjacent continents.

The structural development of the Gorda-Juan de Fuca plate over the last 10 million years can be explained by north-south shortening coupled with the normal tectonism associated with a spreading sea floor.

This hypothesis for the development of the plate is based on the presently known magnetic anomaly pattern. A series of reconstructions of this pattern back through the past 10 million years shows that both the Gorda and Juan de Fuca portions of the plate have grown steadily smaller. The incorporation of sequentially shorter Gorda ridge anomalies into the Pacific plate appears to have led to the northwest-southeast orientation of the Blanco Fracture Zone, with consequent changes in the direction of spreading of the Juan de Fuca Ridge. On the Juan de Fuca portion of the plate, the shortening was accomplished by shear faulting in Cascadia Basin. Furthermore, this faulting resulted in the rapid subduction of this portion of the plate, which, in turn, produced a disconformity in the sediments of Cascadia Basin. The reconstruction strengthens the notion that right lateral strike slip motion between the Pacific and Gorda-Juan de Fuca plate does, indeed, exist.

Sediments and Tectonics of the Gorda-Juan de Fuca Plate

by

James Benjamin Phipps

A THESIS

submitted to

Oregon State University

in partial fulfillment of
the requirements for the
degree of

Doctor of Philosophy

June 1974

APPROVED:

Redacted for Privacy

Associate Professor of Oceanography
in charge of major

Redacted for Privacy

Associate Professor of Oceanography
in charge of major

Redacted for Privacy

Dean of School of Oceanography

Redacted for Privacy

Dean of Graduate School

Date thesis is presented September 5, 1973

Typed by Marjorie Hay for James Benjamin Phipps

ACKNOWLEDGEMENTS

The successful completion of this study is, to a large degree, the result of assistance and encouragement from many people. Drs. Vern Kulm and Ross Heath were my major professors and I especially owe them a debt of gratitude. Dr. Kulm introduced me to the School of Oceanography and provided me with the opportunity to do this study. Dr. Heath has the remarkable quality of finding and providing encouragement in the most trying of situations and to him I am especially indebted.

I was particularly fortunate to be associated with a great class of students and discussions with them helped in the evaluation of the results of the study. In particular, Bruce Malfait and Paul Dauphin were most helpful. Paul also provided me with a home away from home on my many trips to Corvallis which was greatly appreciated. Thanks also are due to Ken Scheidegger and Gary Muehlberg who helped to collect the piston cores used in the study.

I would also like to thank the people at Grays Harbor College who encouraged me to become involved in this study and assisted me in completing it.

Of course none of this would be possible without the support of my family; my parents who are happy to see me complete many years of college, and my wife who is looking forward to a normal household

after being an "oceanography widow" for a long time. To her I owe a special thanks.

Thanks also are due Margie Hay for her typing of the final drafts and to the crew and officers of the R/V YAQUINA for their assistance in gathering the data.

Funding for this study was provided by the National Science Foundation, grants GA-1246 and GA-32122, and by the Office of Naval Research, Contract No. N00014-67-14-0369-0007.

TABLE OF CONTENTS

Table of Contents (continued)

LIST OF FIGURES

List of Figures (continued)

LIST OF TABLES

SEDIMENTS AND TECTONICS OF THE GORDA-JUAN DE FUCA PLATE

GENERAL INTRODUCTION

The Gorda-Juan de Fuca lithospheric plate lies in the Northeast Pacific adjacent to the continental margin of the northwestern United States (Figures 1 and 2). Except for the absence of an obvious trench adjacent to the continental margin, it exhibits most of the characteristics of crustal plates described by Le Pichon (1968) and Morgan (1968). The spreading ridges have produced the classic pattern of magnetic anomalies (Mason and Raff, 1961) that has been explained (Vine, 1966) as representing periods of reversals in polarity of the earth's magnetic field. The concept of transform faulting was developed by Wilson (1965) to explain the fracture zones in the area.

More recent studies of the area deal with sediments (Duncan, 1968; Griggs, 1969; Kulm and Fowler, in press; Kulm, von Huene et al., 1973; Carson, 1973), the continental margin adjacent to the Gorda plate (Spigai, 1971; Silver, 1969), tectonics (Silver, 1969; 1971a, 1971b; Atwater, 1970), and the geophysical aspects (Dehlinger et al., 1970; Tobin and Sykes, 1968; Seeber et al., 1970).

This study is primarily concerned with two kinds of data -- X-ray diffraction analyses of the sediments obtained from cores taken in the area, and continuous seismic profiles that portray the

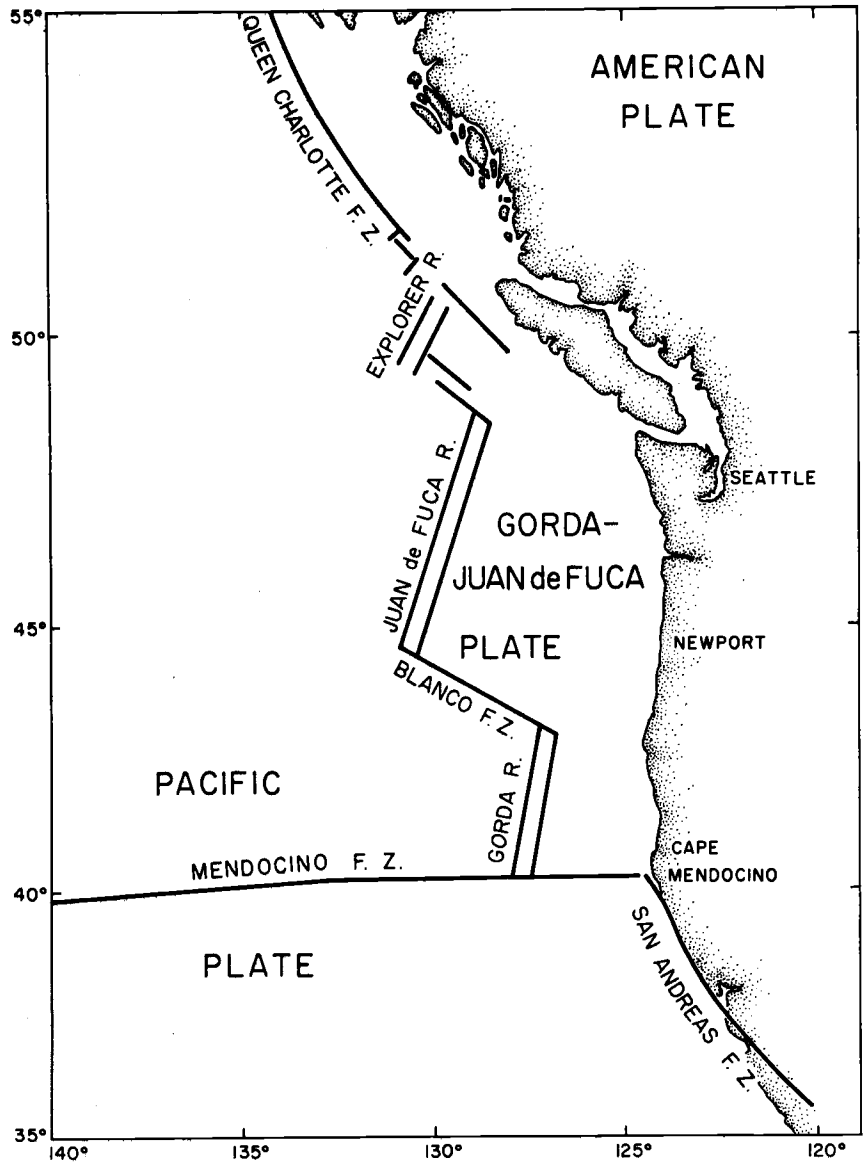

Figure 1. The Gorda-Juan de Fuca Lithospheric plate.

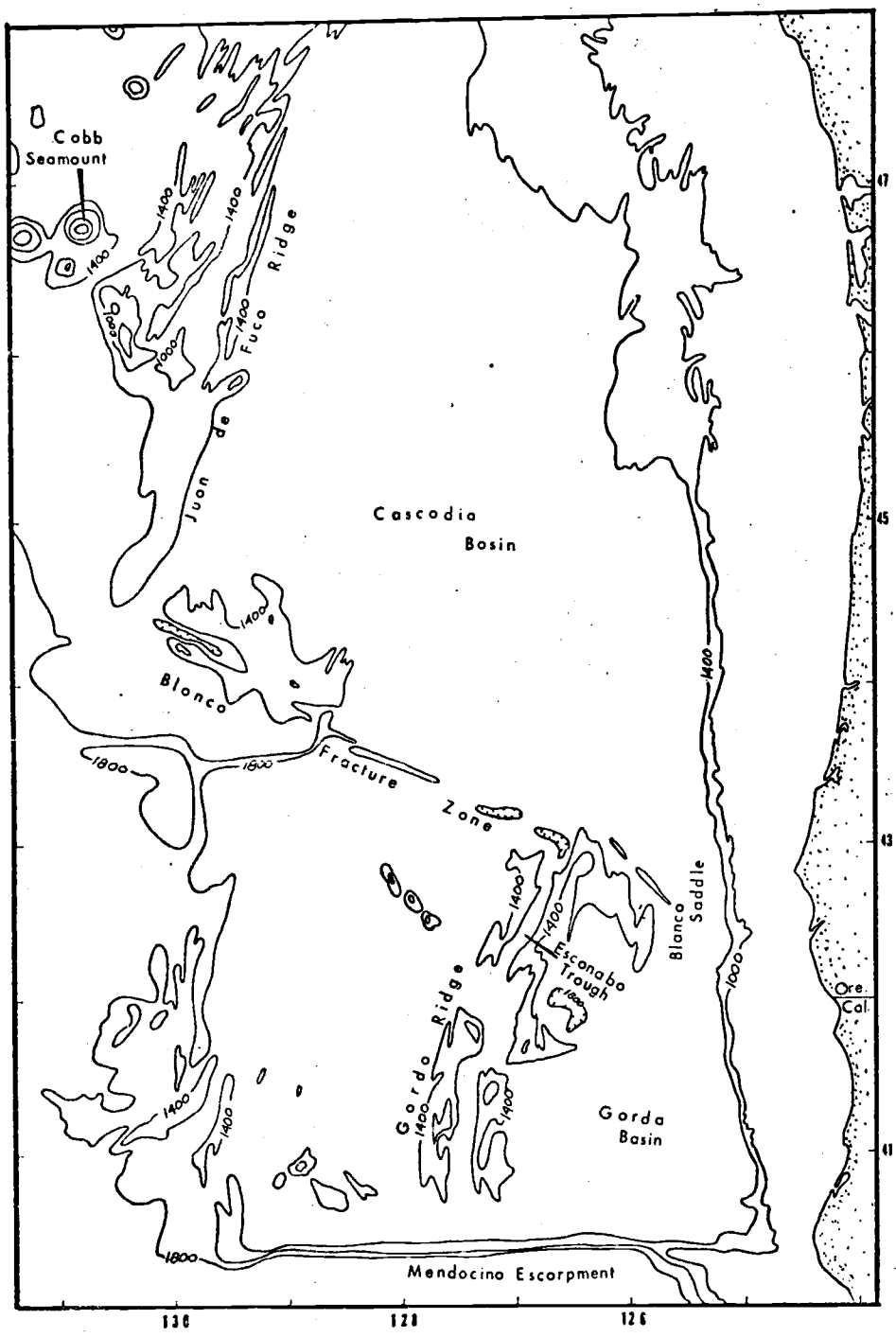

Figure 2. The topography of the Gorda-Juan de Fuca plate. after Chase et al. (1970). The contour interval is 400 fathoms.

gross aspects of the sedimentary column and the topography of the igneous basement rock. The seismic reflection data coupled with earlier geophysical investigations can be used to construct a simple model that explains the development of the present geometry of the Gorda-Juan de Fuca plate.

The X-ray diffraction data show variations in the quartz content of the sediment. These variations appear to reflect both changes in the eolian contribution to the sediment and episodic catastrophic flooding in the Columbia River Basin.

Two factors make the Gorda-Juan de Fuca plate a good area for such a study; the availability of a wealth of older geophysical data that facilitates interpretation of the continuous seismic profiles, and rapid deep-sea sedimentation rates that preserve detailed profiles of the mineral variations during the late Quaternary.

The first portion of the thesis describes variations in the mineral content of the sediments and attempts to relate such variations to late Quaternary climatic and geologic events. The second part of the thesis treats the history of the Gorda-Juan de Fuca plate motions in order to explain the structure of the region.

PART I: SEDIMENTATION

INTRODUCTION

Purpose

The sediments of the Gorda-Juan de Fuca plate have been the subject of several studies dealing primarily with turbidites and channel deposits (Carlson, 1968; Duncan, 1968; Griggs, 1969; Duncan et al., 1970; Silver, 1969; Carson, 1973; Kulm and Fowler, in press). More recent studies by von Huene et al. (1971) and Kulm, vone Huene et al. (1973) are based on data gathered during Leg 18 of the Deep Sea Drilling Project. The pelagic sediments of the area have been little studied, and there are no studies of the mineralogy of the silt sized fraction. Because studies of silt mineralogy over a broader area (Windom, 1969; Rex and Goldberg, 1958) suggest that 2 to 20 micron material is the dominant size fraction of eolian sediment, the initial study of this size fraction was undertaken in an attempt to identify late Quaternary variations in the eolian contribution of sediment to the area.

A study of the clay size fraction was undertaken to extend the work of Duncan et al. (1970) to the ridge areas. The coarse fraction (> 62 micron) of the sediment was examined to establish a biostratigraphic framework within which to interpret the mineralogical data.

Sample Collection and Processing

The sediment samples used in this study were collected on cruises of the R/V YAQUINA during 1968, 1969 and 1970. All the cores were taken with a modified Ewing piston corer using a multiple corer (Fowler and Kulm, 1966) as a trip weight. The cores were collected in clear plastic liners and kept in cold storage until processed. Core processing has been described in detail by Griggs (1969) and Duncan (1968).

Initial studies suggested that a one-meter sample interval would adequately define sediment variations resulting from major changes in late Quaternary climate (Shackleton and Opdyke, 1973). A sedimentation rate of approximately 10 cm/1000 years for the area, which was used to establish the one-meter sample interval, was determined from carbon-14 data.

For each sample, the clay ($< 2\mu$ fraction) and silt (2 to 20 μ fraction) mineralogy was determined by X-ray diffraction. The coarse fraction ($> 62\mu$) was examined with a binocular microscope to determine the radiolarian-foraminiferan ratio for stratigraphic control (Duncan, 1968). Figure 3 shows the steps involved in sample processing.

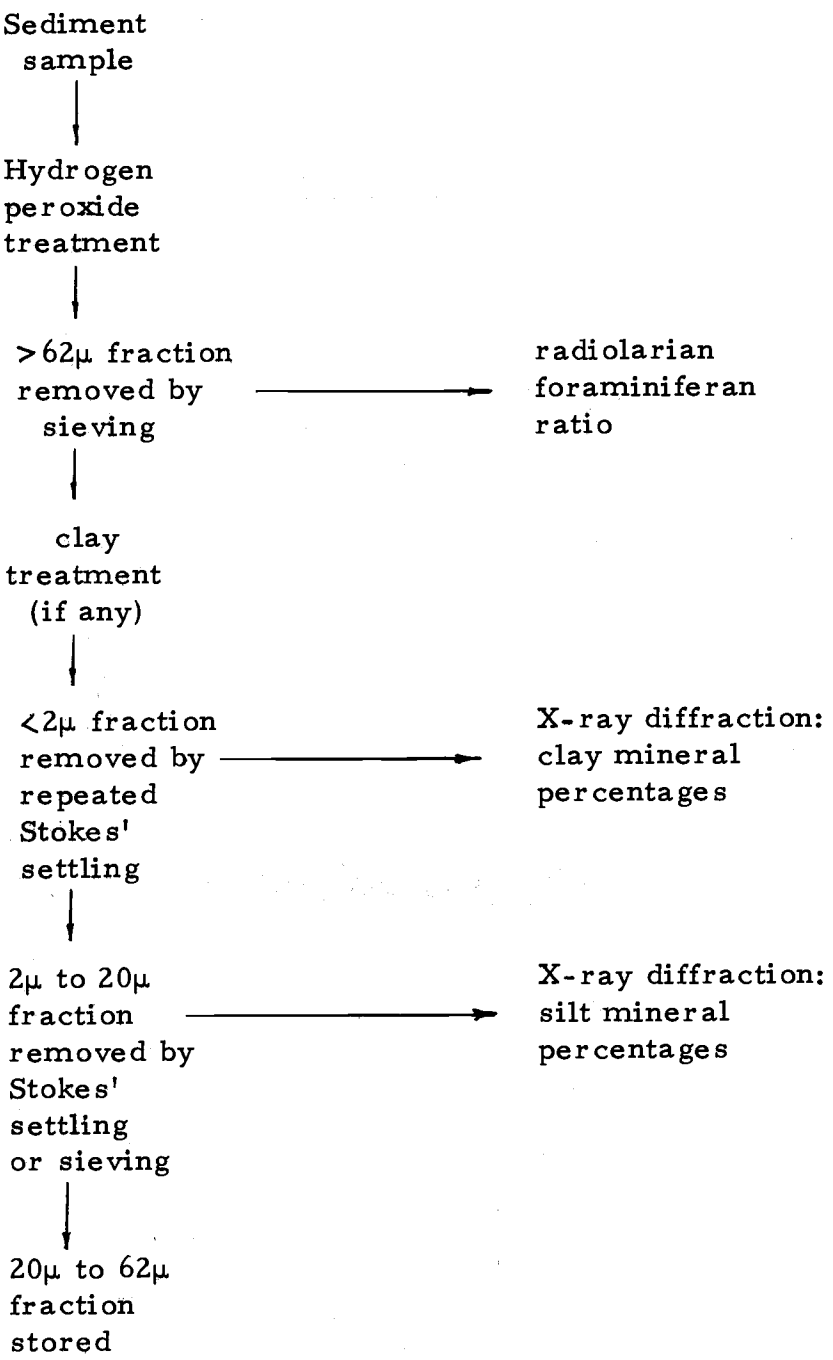

Figure 3. Flow sheet of laboratory operations.

REGIONAL DISTRIBUTION AND SOURCES OF SEDIMENT

Sediment Distribution

The distribution of pelagic and turbidite sediments on the Gorda-Juan de Fuca plate is shown in Figure 4. From this illustration it is obvious that the pelagic sediment of the area appear as "islands" in a predominately turbidite-covered sea floor. The terms "turbidite" and "pelagic sediment" are defined, for the purposes of this report, from the character of the sedimentary layers in the continuous seismic profiles. Following Hamilton (1967), turbidites are defined by their numerous reflectors and generally horizontal layering whereas pelagic sediments are acoustically transparent and conform, more or less, to the underlying basement topography.

Some of the turbidites were sampled at the far western side of the Cascadia Basin and were found to be very similar to cores from the area described by earlier workers (Duncan, 1968; Griggs, 1969; Spigai, 1970; Horn, 1969). The deposits consist of gray and olive gray lutites with interbedded sands and silts. In cores 6908-5 and 6808-4 there are, in addition, interbeds of foraminiferal lutite (Duncan, 1968). These beds of foraminiferal lutite are characterized by a high content of pelagic foraminifera, an oxidized yellow color, gradational contacts with the underlying pelitic portion of the

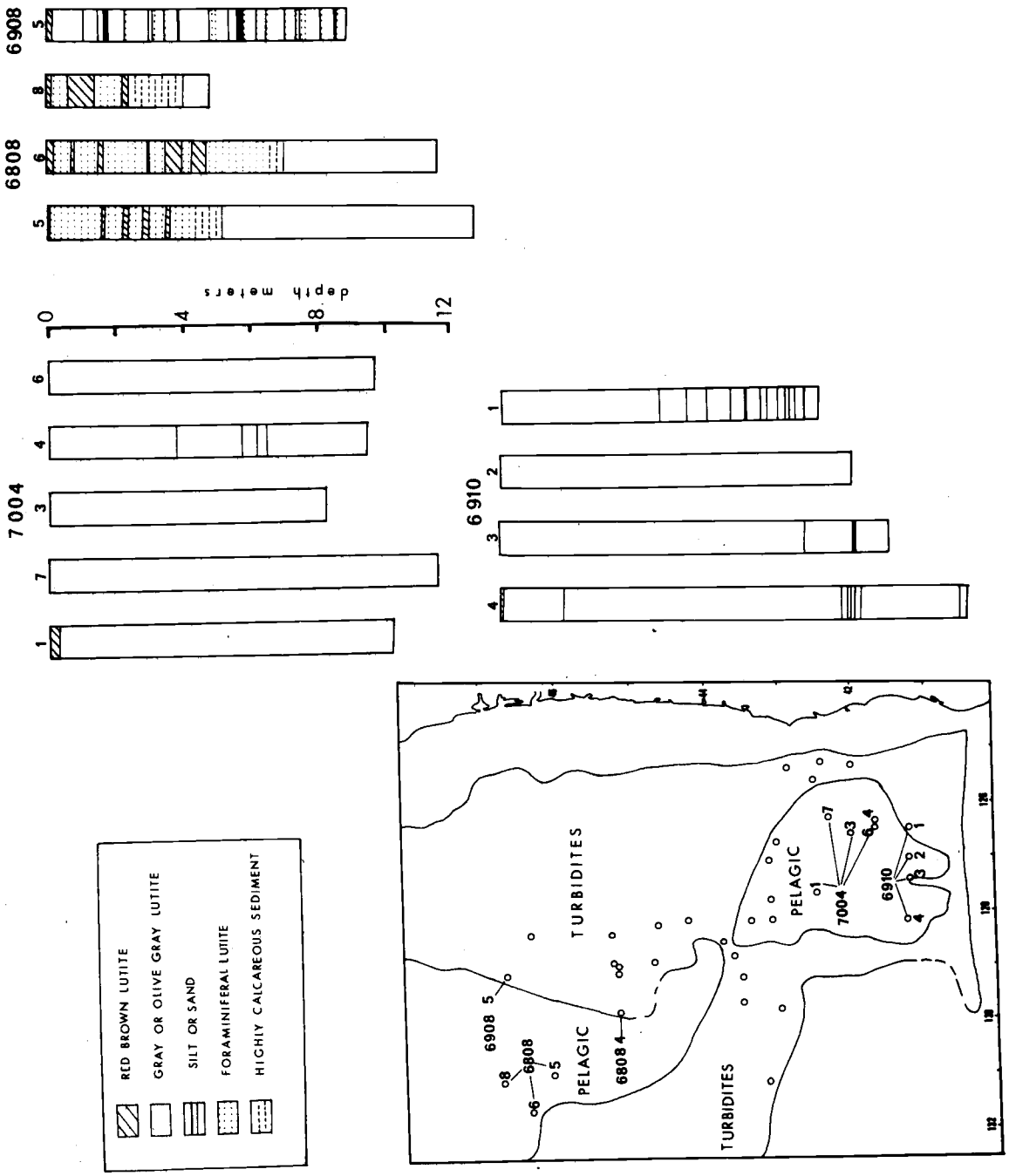

Figure 4. The regional distribution of sediment types on the ridges and adjacent basins. The numbered cores are those used in the study. Designation of turbidites and pelagic sediment is, in part, from Horn et al. (1970).

turbidite flow and a sharp erosional contact with the basal units of the overlying flow. These data suggest that foraminiferal lutites accumulated very slowly during periods of time between turbidite flows.

To the west of the essentially sediment-free Juan de Fuca Ridge crest is an "island" of pelagic sediment. The western flank of the ridge is covered with biogenous-rich sediments containing abundant foraminifera and coccoliths. The mineral fraction of this sediment is commonly oxidized to a reddish brown color which contrasts with the olive gray color that predominates in the other cores.

Pelagic sediments also cover the Gorda Ridge area where, like those of the Juan de Fuca Ridge, they are surrounded by turbidites. Cores in this area consist of monotonous, unstructured, olive gray lutite with occasional mottles and numerous fecal pellets (Figure 4). These cores appear to contain the most complete late Quaternary pelagic sequence from the area.

Sediment Sources

There are a number of possible sources for the deposits of the Gorda-Juan de Fuca plate: the adjacent continent; dust from the prevailing westerlies; "nepheloid layer" introduction from other parts of the sea floor; and volcanic debris from within the plate.

A continental source of the turbidites has been convincingly

demonstrated (Carlson, 1967; Nelson, 1968; Duncan, 1968; Griggs, 1969; Carson, 1971). The pelagic sediments, too, are probably derived from the adjacent continent as their sedimentation rates (about 10 cm/1,000 years) appear too great to be attributed to the other possible sources.

Dust from the prevailing westerlies is deposited over the entire plate, but the eolian sedimentation rate (about 1 mm/1,000 years) is much lower than continental sediment deposition rates. In the 2 to 20 micron size fraction, however, the eolian sedimentation rate forms a significant portion of the total rate in this size range.

A comparison of the upper pelitic zones of turbidite flows (deposited rapidly) with the overlying foraminiferal lutite (deposited slowly) shows that the foraminiferal lutite is enriched in 2 to 20 micron size quartz relative to the pelitic zone (Table 1). Because dusts at this latitude are quartz-rich in the same size fraction (Rex and Goldberg, 1958), it is logical to attribute the quartz enrichment of the foraminiferal lutites to eolian deposition.

The eolian sediment presently falling on the area was sampled directly with a nylon mesh kite (Parkin et al., 1970). The kite was flown for about ten hours during April, 1970. Despite the short sampling time, the character of the dust recovered supports the work of Windom (1969) who found that the calcium-carbonte-free fraction of North American dust consists of feldspar, quartz,

Table 1. Comparison of the pelagic and pelitic sediments of core 6908-5 from the western side of the Cascadia Basin.

Sample Number	Depth in the Core	Description	% Quartz
33	124 cm	pelagic	37
34	135 cm	pelitic	30
42	350 cm	pelagic	54
43	365 cm	pelitic	49
45	540 cm	pelagic	46
46	560 cm	pelitic	42

	Pelagic	Pelitic	D	$(D-\bar{D})^2$
Pair 1	37	30	+7	2.89
Pair 2	54	49	+5	0.90
Pair 3	46	42	+4	1.69
$\bar{x}$	45.6	40.6	5.3	

$S_D = 2.74$ $S_{\bar{D}} = 1.58$ $t = 3.35$

Ho: $\mu_D = 0$

t is significant at the 10% level

Ho is rejected

There is a significant difference in the amount of quartz in the pelagic and pelitic samples.

amphibole, chlorite and mica. Diffractograms of the dust and deep sea sediment are shown in Figure 5. Unfortunately, no relative concentration values could be determined for this samples, as it was so small that it had to be X-rayed as an oriented sample on a silver plug. This procedure prevents the comparison of peak intensities used for the rest of the silt samples.

Although no sample of pure volcanic sediment was available from the area, the coarse fraction of core 6910-3 is rich in volcanic glass shards, indicating the presence of volcanic debris. The clay and silt fraction of this core are mineralogically indistinguishable from sediment from nearby glass-free cores (Appendix 1). It is concluded that the volcanic input of sediment to the area is not recognizable in the size fractions studied.

Rates of sedimentation due to influx of "nepheloid layer" material carried by slowly moving bottom waters are unknown. Based on total sedimentation rates in areas of the North Pacific far removed or shielded from continental influences, however, it appears that the nepheloid contribution is comparable to the eolian input. In elevated areas, like those from which the Gorda-Juan de Fuca pelagic cores were obtained, the nepheloid contribution to the sediment is probably undetectable. Dauphin's (1972) study of the size distribution of quartz supports this conclusion.

Thus, it seems that the dominant sediment source for the

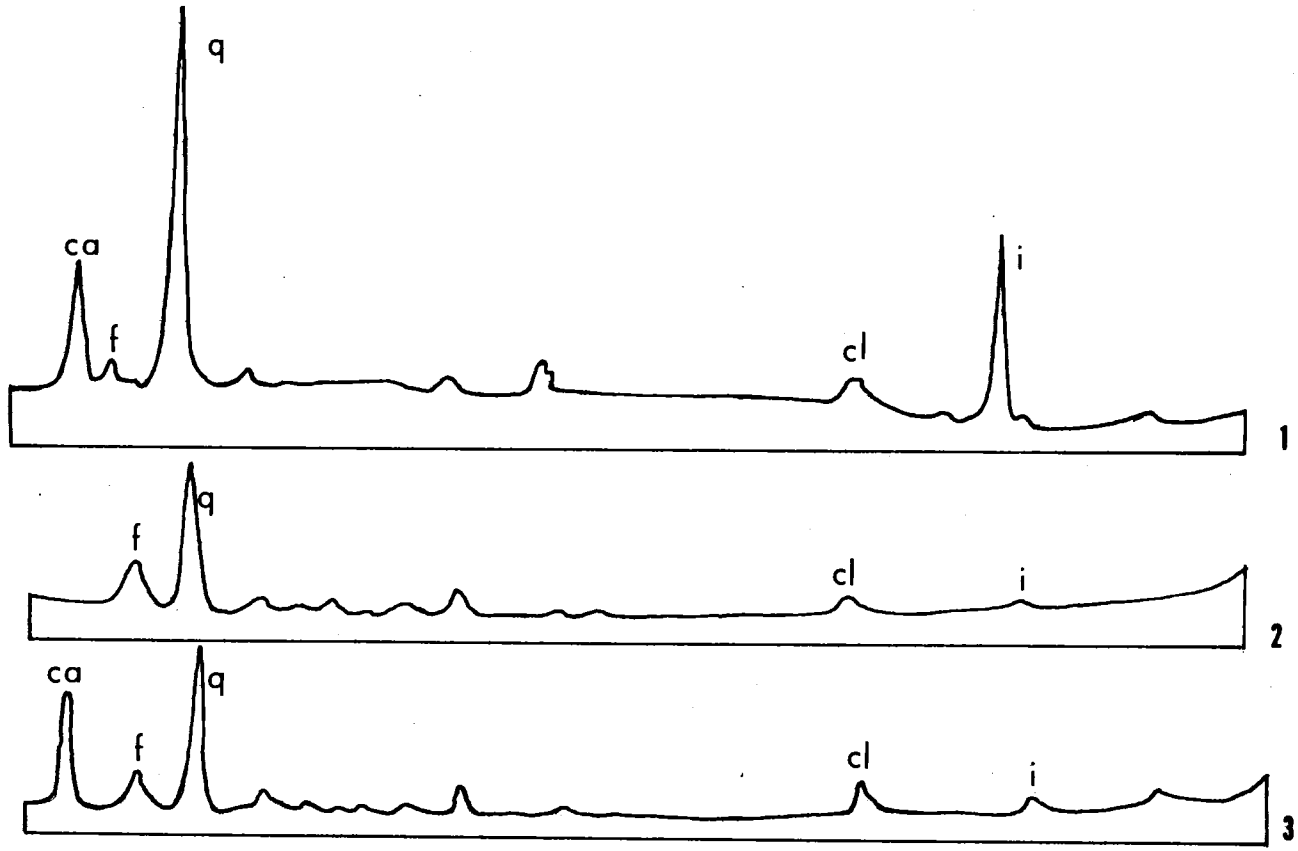

Figure 5. A comparison of diffractograms of the silt fractions of eolian and core samples from the Gorda Ridge. 1 is a sample of dust from the Gorda Ridge area. 2 and 3 are typical diffractograms from the sediments of the Gorda Ridge area. Ca = calcite at 29.3° 2θ, f = feldspar at 27.7° 2θ, q = quartz at 26.7° 2θ, cl = chlorite at 12.4° 2θ, i = mica at 8.8° 2θ.

Gorda-Juan de Fuca plate is hemipelagic deposition from the adjacent continent, with a minor input of eolian material.

FORAMINIFERAN-RADIOLARIAN RATIO

The > 62 micron fractions of the samples were examined microscopically to determine foraminiferan-radiolarian ratios. To obtain the ratio, a split of the coarse fraction was spread on a gridded slide and a minimum of 200 tests were counted with the aid of a binocular microscope. Duncan (1968) demonstrated that the fauna preserved in the sediment of the Cascadia Basin and adjacent areas changed from dominantly radiolaria to dominantly foraminifera about 12,500 years ago. He suggested that this change defines the boundary between the Holocene and Pleistocene in this area. The possibility that this Holocene boundary is time transgressive from deep to shallow water (Barnard and McManus, 1973) does not affect the synchroneity of the boundary in the study area, as all of the core sites are in deep water.

This faunal change is found in the upper portions of the Gorda Ridge as well as Cascadia Basin cores. The closely spaced samples from core 6910-2 even show (Figure 6) the less well-defined intervals of increased radiolarian abundance that occur at 16,000-18,000 and 25,000-28,000 years B. P. (Duncan et al., 1970). In addition, a similar event occurs in most of the Gorda Ridge cores at a depth of

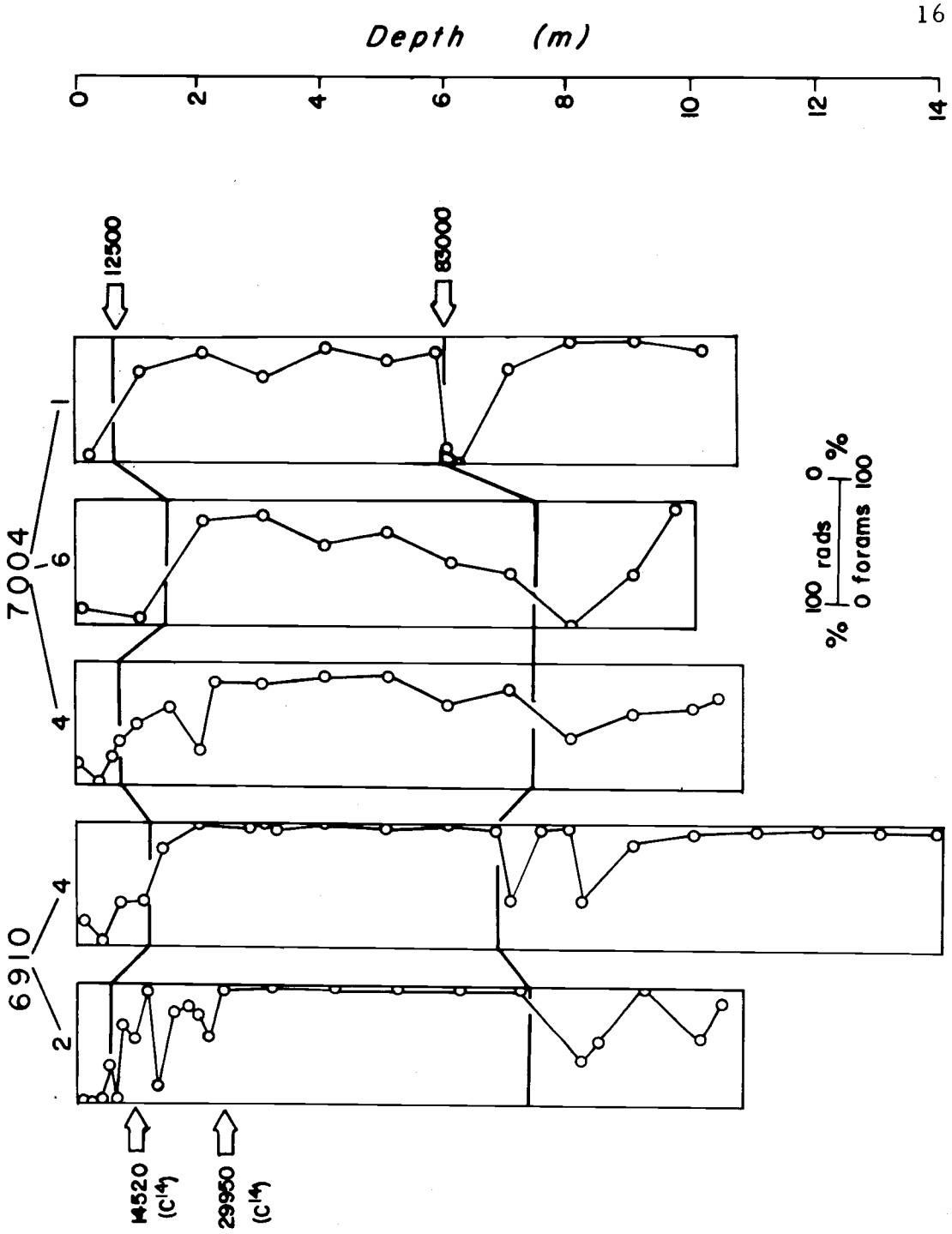

Figure 6. Relative abundances of radiolaria and foraminifera in cores from the Gorda Ridge. Ages of the faunal datums appear on the right and the carbon-14 dates in core 6910-2 on the left.

7 to 8 meters (Figure 6). It is tentatively dated as approximately 83,000 years B.P. in core 6910-2 by extrapolating sedimentation rates determined by carbon-14 dating.

The higher relative rates of accumulation of radiolaria in the Holocene sediment could reflect at least two factors: changes in composition of the zooplankton; or selective dissolution of the foraminifera tests in the water column and uppermost few centimeters of the sediment (Peterson, 1969; Berger, 1971; Duncan et al., 1970). Duncan et al. (1970) argue that dissolution of foraminifera could not be responsible for the trends they describe. Their data suggest that the radiolarian-rich sediment forming the upper portions of the cores may result at least in part from changes in the surface zooplankton.

In the Santa Barbara Basin, Berger (1971) reports that only 15% of the planktonic foraminifera are preserved in the sediment, due to dissolution. The high rate of dissolution results from an abundance of organic carbon in the area. The organic matter oxidizes to produce CO_2 which reacts with the calcite tests. Duncan (1968) noted a large increase in the amount of organic carbon in the Holocene sediment compared to late Pleistocene. This increase in organic matter occurs at the same time as the faunal change. The synchroneity of the increase of organic carbon and the disappearance of the foraminifera from the sediment in a number of cores suggests that dissolution of the foraminiferal tests may well be a factor in the 12,500 year

faunal change.

Many of the samples examined during this study that are rich in radiolaria contain few, if any, foraminifera. Those present are usually rugose benthic forms that constitute the least soluble fraction of pelagic assemblages.

Despite the uncertain cause of the faunal changes, their occurrence at 12,500 years and 83,000 years provides an easily recognizable pair of biostratigraphic datums for this study.

X-RAY MINERALOGY

Clay Size Fraction

Preparation of Samples

Prior to X-raying soil or sediment samples, many workers selectively remove components such as free iron, manganese, and calcium carbonate that tend to mask the crystalline phases of interest (Heath, 1968). A study of 19 paired samples from different depths in core 6908-5 suggests that such pre-treatments (Figure 7) produce no significant improvement in the precision of clay mineral determinations (Table 2).

The samples of this study were first treated with hydrogen peroxide. The clay fraction was then separated from the rest of the sample by allowing the sediment to settle through a column of water

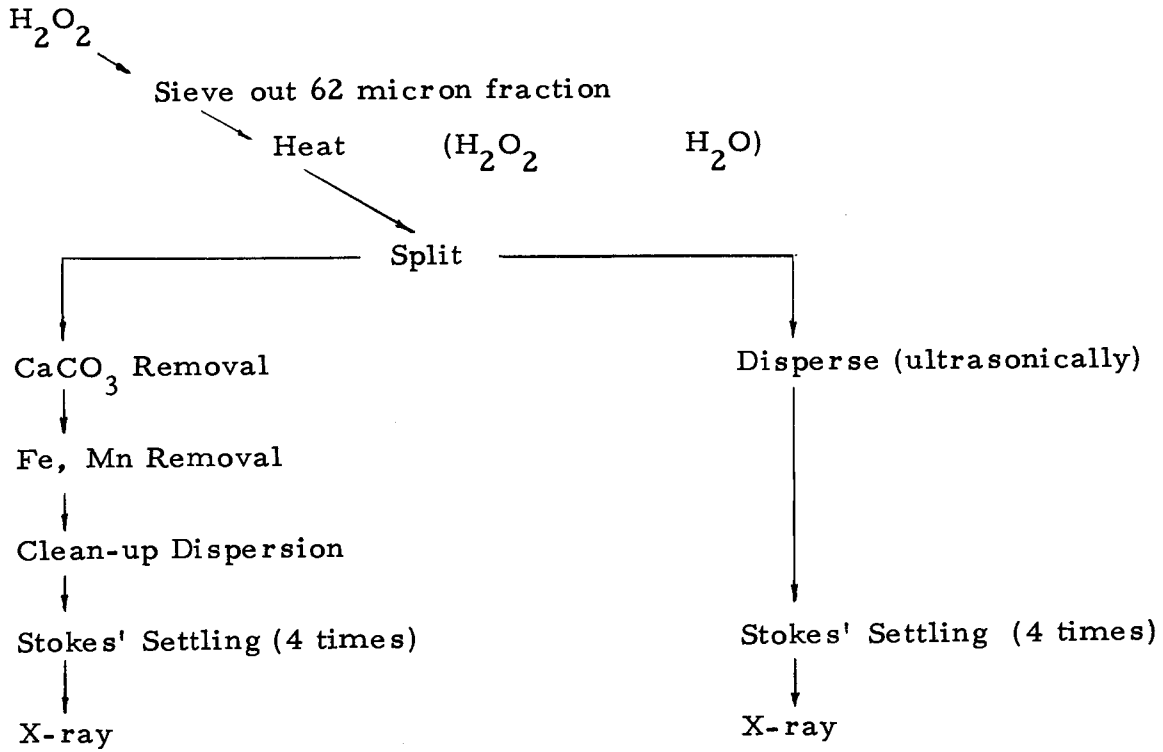

Figure 7. The difference in treated clays (on the left) and untreated clays (on the right). Flow sheet of preparations of untreated (on the right) and chemically cleaned clays (on the left).

Table 2. A comparison of the mineralogy of treated and untreated samples. The sum of the difference (D) is 15 with a standard deviation of 3.9. A students-t test shows that the null hypothesis that the mean of the differences ($\bar{D}$) is equal to zero cannot be rejected.

		Concentrations					
		Treated Samples			Untreated Samples		
Sample Number	Depth (cm)	S%*	I%*	C%*	S%	I%	C%
31	9	34	33	33	31	39	30
32	32	33	36	30	35	39	26
33	124	30	34	35	36	34	30
34	135	30	36	34	33	36	31
35	145	30	35	36	25	40	35
36	155	32	31	37	34	35	31
37	165	35	29	36	34	33	33
38	190	30	31	39	32	31	37
39	200	32	27	41	30	33	38
40	210	30	29	41	30	31	38
41	220	30	38	32	29	32	39
42	350	27	50	23	29	50	20
43	365	33	36	31	32	32	36
44	380	36	29	35	31	32	37
45	540	32	33	35	38	32	29
46	550	25	43	32	27	34	39
47	560	23	34	43	27	36	38
48	825	21	44	36	18	45	37
49	845	15	49	36	22	45	33
	$\bar{X}$	29.36	35.63	35.0	30.15	36.5	33.5
	σ	5.2	6.6	4.5	4.8	5.4	5.0

* S = Smectite

I = Illite

C = Chlorite

Table 2, continued:

A comparison of the Differences Between Treated Smectites (St) and Untreated Smectites (Su).

	St	Su	D	$(D-\bar{D})^2$
Σ			15	278.54
$\bar{X}$	29.37	30.15	$.79=\bar{D}$	

Df = 18 $S_D = 3.9$ $S_{\bar{D}} = .90$ t = .8777 (not significant)

Ho: $\mu_D = 0$ cannot be rejected.

There is no difference between treated and untreated smectite samples.

for an appropriate time computed from Stokes' Law. The fines, still in suspension, were decanted off and the process repeated until the decanted suspension became clear.

The suspension was concentrated by candle filtering. The addition of a few drops of dilute sodium hexametaphosphate (Calgon) and agitation with an ultrasonic energy probe helped to disperse the suspension.

The concentrated suspension was pipetted onto a porous silver plug and the fluid removed with the aid of a vacuum, leaving the clays lying with their basal layers parallel to the flat upper surface of the plug. After one hour's drying the plug was sprayed with magnesium saturated glycerol to expand the smectites and was further dried for at least 45 minutes before X-raying.

The clays were scanned from 2 to 14 degrees 2θ on a Norelco diffractometer with the following settings: tube current, 25 ma; voltage, 35 kv; monochromatized copper radiation; divergence silt 1°, receiving silt 0.1 mm; scale factor 1×10^3; scanning speed 1° per minute; time constant 4 seconds; and strip chart recorder, 1 inch per minute.

Results

With very few exceptions all of the samples contained the same minerals, smectite expanded to 17Å, illite to 10Å and chlorite at 7Å.

The identity of these minerals at these peaks corresponds to the work of Duncan (1968). Occasional checks (Biscaye, 1964a) were made to verify the lack of kaolinite noted by other workers in the area (Duncan, 1968; Griffin et al., 1968).

The chlorite and illite peaks were consistently sharp and well-defined in contrast to the smectite peak which formed a low shoulder between the sharply descending baseline and the 001 chlorite peak.

The percent of clay components were calculated using Biscaye's (1965) technique, which has been used by others in this area (Griggs, 1969 and Duncan, 1968). The assumption is made that the identified clay minerals on each trace total 100%. The areas under the mineral peaks are multiplied by weighting factors: one times the 17Å smectite peak; four times the 10Å illite peak; and two times the 7Å chlorite peak. The fraction of each mineral is obtained by dividing its weighted peak area by the sum of the weighted areas.

Precision of the Results

Because there are few piston cores from the area of interest, each must be treated as a valid sample of a rather large area. In order to test the combined effect of areal variations and treatment effects on mineralogy, a single experiment was conducted. Seven cores taken on both flanks of the Gorda Ridge (Figure 8) in conjunction with heat flow studies were sampled at a constant depth and

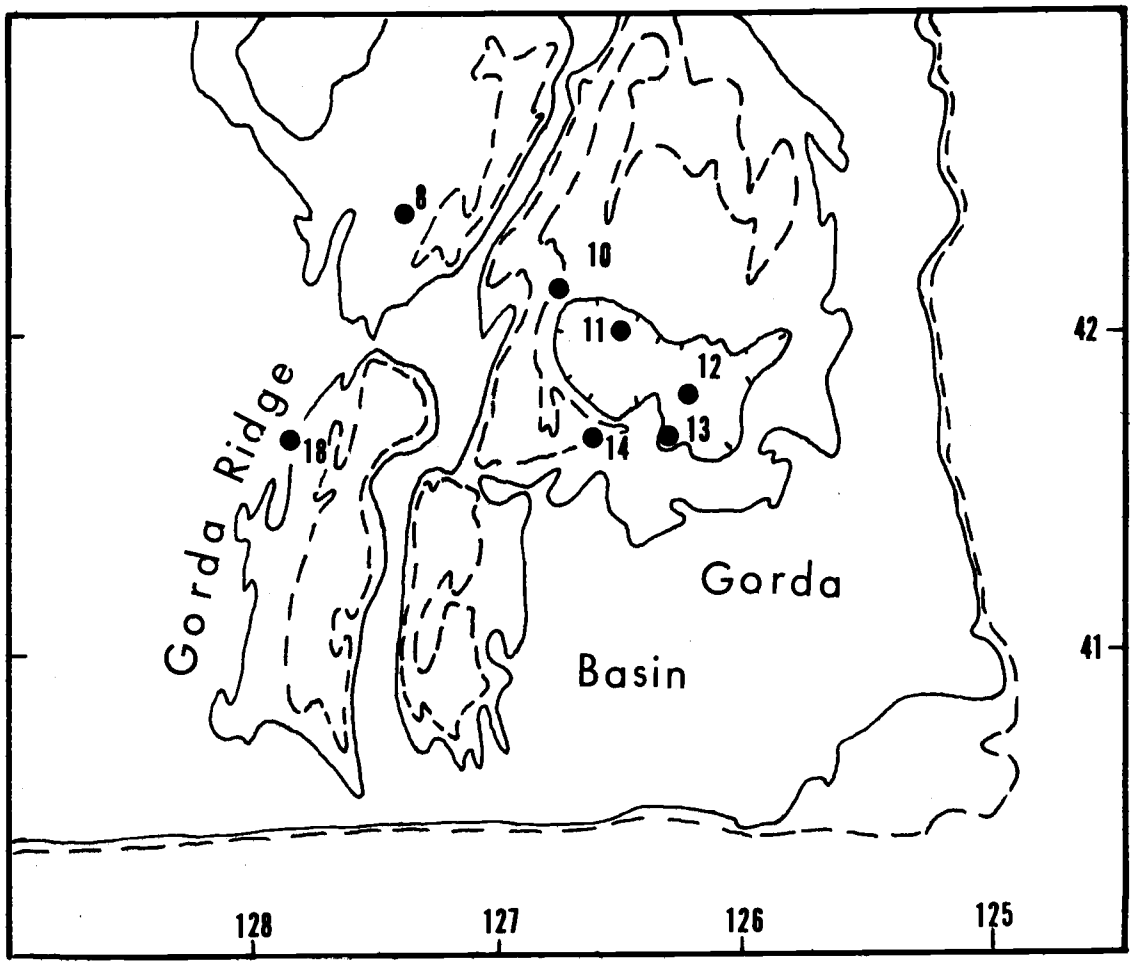

Figure 8. Chart of the location of the thermoprobe cores used to test the mineralogical analyses. The solid contours are 1400 fathoms and the dashed contours are 1200 fathoms.

mineralogically analyzed exactly like the rest of the samples in the study. Table 3 shows the results of the experiment. The greatest variation in the clay minerals was in the chlorite with a standard deviation of 4.4%. The standard deviation for smectite was only 1.9%. Thus, changes in the clay mineral content of the cores can be considered representative of large areas, within the constraints of these statistical variances.

Interpretation of Results

All $< 2\mu$ samples contain smectite, illite and chlorite only. Thus, all variations in the clay composition reflect variations in the relative concentrations of these three components. It was somewhat surprising to discover how small are the variations in mineralogy of the clay-sized fraction in this study as compared to the variations in clay mineral concentrations that occur nearer the mouth of the Columbia River (Duncan, Kulm and Griggs, 1970).

The gross variations in the clay mineral distribution are shown in Figure 9. These plots of the average mineralogy of whole cores show three distinct groups labeled A, B and C.

The sediments of the group-A cores are relatively smectite-rich turbidites. Similar turbidites on the eastern side of the Cascadia Basin contain even higher smectite values (Duncan et al., 1970). The groups B and C sediments are predominantly pelagic (as defined in

Table 3. Precision of mineralogical analyses of silt and clay size fractions. The body of the table is the percent concentration of the various minerals.

sample number	21	22	23	24	25	26	27			
core number	T-8	T-10	T-11	T-12	T-13	T-14	T-18			
sample depth	10	12	10	10	10	10	5			
Clay size								σ	$\bar{X}$	95% C.I.
Smectite	21	16	17	18	20	20	20	1.9	18.8	20.6 - 17.1
Illite	44	41	43	43	49	40	40	3.1	42.7	45.6 - 39.8
Chlorite	35	42	40	32	31	40	40	4.4	37.1	41.22 - 33.1
Silt Size										
Plagioclase	19	18	21	19	20	20	19	1.0	19.4	20.3 - 18.5
Quartz	50	52	52	50	47	52	50	1.8	50.4	52.1 - 48.7
Chlorite	21	22	20	22	24	22	23	1.3	22.0	23.2 - 20.8
Mica	9	8	6	10	8	6	8	1.5	7.8	9.2 - 6.5

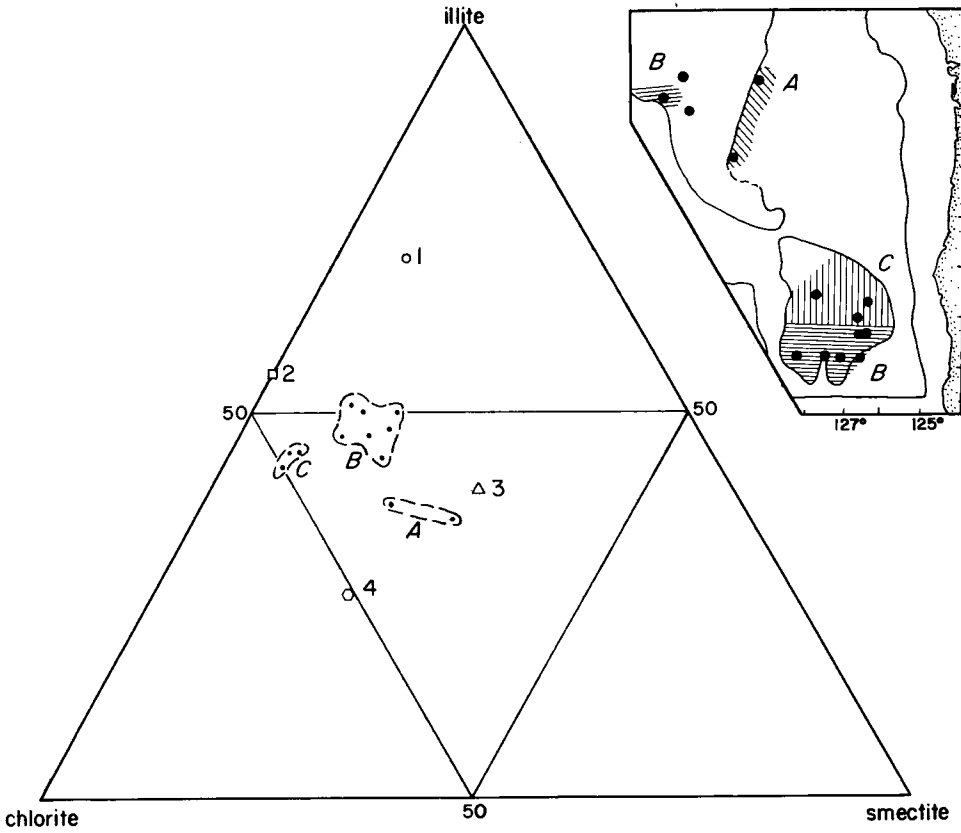

Figure 9. A ternary diagram showing the whole core averages of chlorite, smectite, and illite from the Gorda-Juan de Fuca plate. Distinct groups are lettered A, B, C, and the possible end points are numbered: 1, Upper Columbia River Basin sediment; 2, dust collected on Mt. Olympus (Windom, 1969); 3, the mean composition of Pleistocene sediment in Cascadia Basin (Duncan, 1968); and 4, is Klamath Mountain sediment (Duncan et al., 1970). The map is taken from Figure 4 and shows the location of the clay mineral groups.

this report) and lower in smectite content. The low smectite content is consistent with the concept of eolian enrichment of ridge flank sediment, which will be further discussed in connection with the silts.

The sediments of groups B and C are similar in terms of lithology (both are pelagic) and physiographic location (both are on ridge flanks). Group C sediments are closer to the latitude of the Rogue River, which carries a clay mineral suite of 23% smectite, 26% illite and 51% chlorite (Duncan et al., 1970). It is tempting to suggest that the group C clays show the influence of Rogue River sediment, while group B does not. Unfortunately, neither known current patterns nor distance of individual sites from the Rogue support such a hypothesis. It appears that the clay mineral distribution in the Gorda Ridge area is complex enough to prohibit a simple explanation of the distribution pattern with the density of core coverage now available. The work of Fowler and Kulm (1970), who report chlorite-rich and chlorite-poor clays from sedimentary rocks dredged from the ridge crest near 41°15' latitude suggests that the complexity is not only a recent phenomenon.

Silt Size

Preparation of Samples

The 2 to 20 micron silt fraction was separated from the

remainder of the sample by repeated Stokes' settling (explained above) or by sieving with the aid of an ultrasonic probe. The use of ultrasonic energy to prevent the 20 micron sieve from clogging greatly speeds the size fractionation process.

After the size separation was completed the samples were dried at 90° C and then pressed into a planchet to be X-rayed. The machine and settings were similar to those used for the clays with the exception of an increased scale factor (to 2×10^3) and an increased scan (from 2° to 37° 2θ).

Results

The diffractograms reveal the dominance of four minerals; feldspar, quartz, mica and chlorite in all samples. Note that the 10Å peak is labeled mica in the silt fraction while the same peak is called illite in the clay size fraction. A semi-quantitative estimate of the relative concentrations of these minerals was made by the method described by Rex (1970). In this method, each mineral is identified and its abundance estimated from the character of its primary peak on the diffractogram.

The percentage concentrations of these minerals were calculated using these peak heights, adjusted for the interference of secondary peaks of other minerals, multiplied by calibration factors and summed to 100%.

For this study the following peaks were used: feldspar 27.35 - 28.15; quartz 26.45 - 26.95; mica 8.50 - 9.20; and chlorite 11.60 - 12.80 degrees 2θ. Note that the chlorite peak used in this work was the larger 002 peak rather than the 001 peak used by Rex (1970) in his Deep Sea Drilling Project work. This results in higher chlorite values (and lower quartz, feldspar, and mica values) in this work than would be estimated by Rex (1970). For example, the average mineral concentrations of the samples from core 6910-2 changed by +4% feldspar, +10% quartz, -16% chlorite and +2% mica by using the 001 rather than the 002 chlorite peak height in the calculations.

It is important to note that, due to this, as well as the possibility of amorphous material affecting the peak size, the percent concentrations are relative, and may differ substantially from absolute values.

Precision of Results

The same heat-probe core samples that were used to determine the precision of the clay mineral data were used to determine the precision of the silt data. The isolation of the silt-size fraction as well as the sample treatment were identical to those described earlier in the thesis. Table 3 shows the results of the study. The greatest variation was in the quartz which had a standard deviation of 1.8% and a 95% confidence interval of $\pm$ 1.7% for the mean.

Interpretation of Results

The 2 to 20 micron fractions of the samples studied is dominated by four minerals: feldspar, quartz, chlorite, and mica, which average 19%, 50%, 23%, and 8%, respectively, of the size fraction. Variations in the concentrations of these minerals with depth are shown in Figure 10. It is noteworthy that the variations in the quartz content correlate negatively with the chlorite concentrations. A high percentage of quartz is matched by a low percentage of chlorite. This may be largely induced by the summing of the concentrations to 100% (Chayes, 1960), although the feldspar and mica concentrations do not exhibit this negative correlation. Thus, the variation in the relative amount of quartz is the dominant feature of the mineral concentration data. Note that if the 001 chlorite peak were used in the calculations, the dominance of quartz over the other minerals would become even greater.

The turbidites of cores 6808-4 and 6908-5 show an erratic distribution of quartz within each flow (Appendix 1) and an overall slightly lower quartz content (average 44% for core 6908-5) than the pelagic sediments of the Gorda Ridge.

The most striking results come from the analyses of the sediments from the Gorda Ridge area. The cores in this area contain alternating zones (labeled L, M, N, and O) that are relatively enriched and depleted in quartz, and can be correlated over the entire

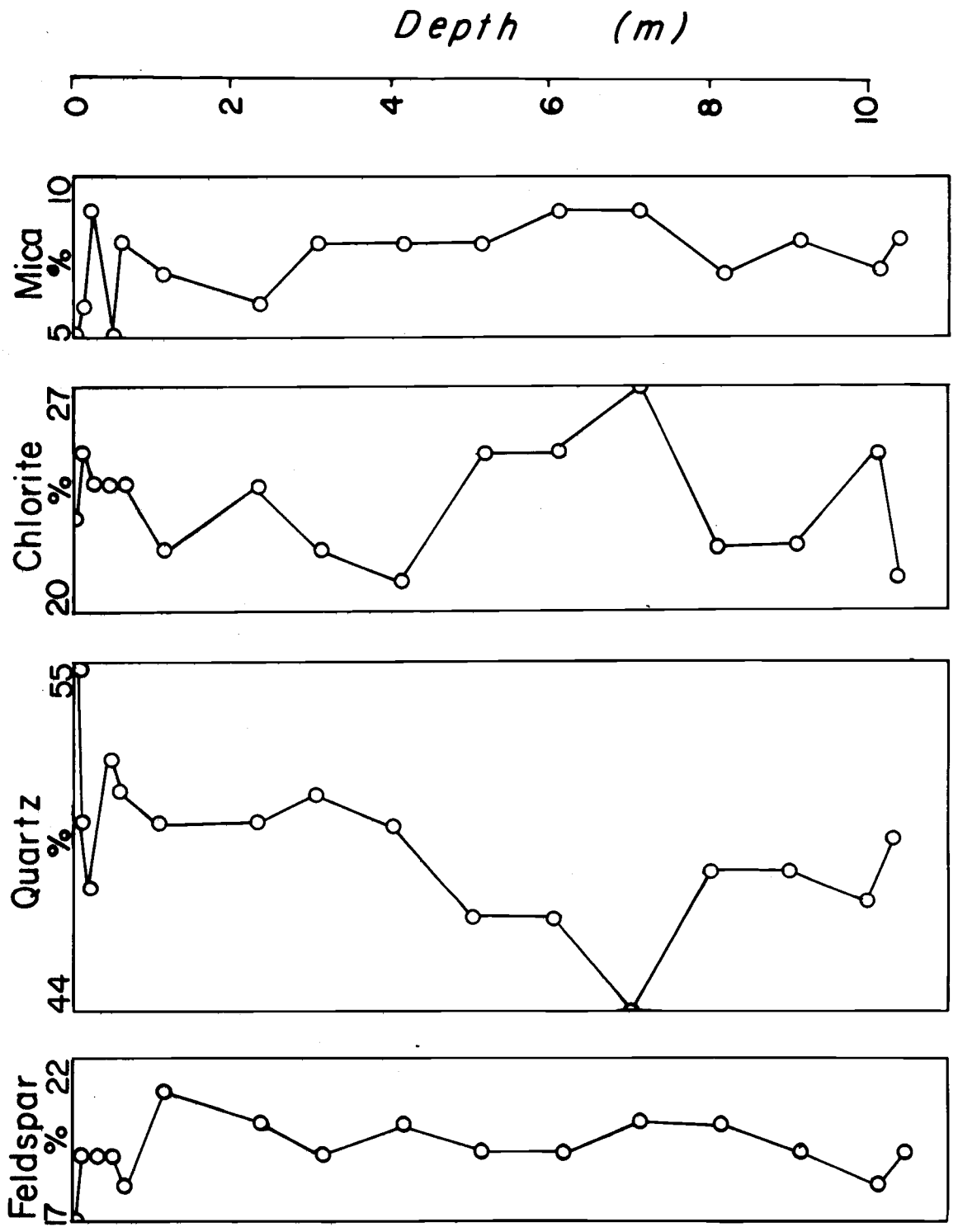

Figure 10. The silt mineralogy of core 6910-2.

area (Figure 11).

These zones appear to be synchronous over the entire Gorda Ridge area, suggesting that they result from a large-scale process affecting sedimentation of the entire area. The data suggest that the process is one of periodic quartz enrichment of the normal pelagic sediment.

DISCUSSION

Significance of Biostratigraphic and Mineral Datums Agreement

The 12,500 year biostratigraphic datum based upon foraminiferan-radiolarian ratios has been recognized and dated over much of the Gorda-Juan de Fuca plate (Duncan, 1968). The cores studied in this report contain this 12,500 datum as well as a similar older one, tentatively dated as 83,000 years old. When these datums are plotted on the abundance curves for 2 to 20 micron quartz they parallel boundaries between intervals of high and low quartz abundance, here called mineral datums (Figure 11).

The mineralogic and biostratigraphic datums are found in the same relative positions from core to core. Because they are independent variables (the abundance of microfossils in no way directly affects the abundance of 2 to 20 micron quartz), the agreement between them supports the idea that the processes that led to their

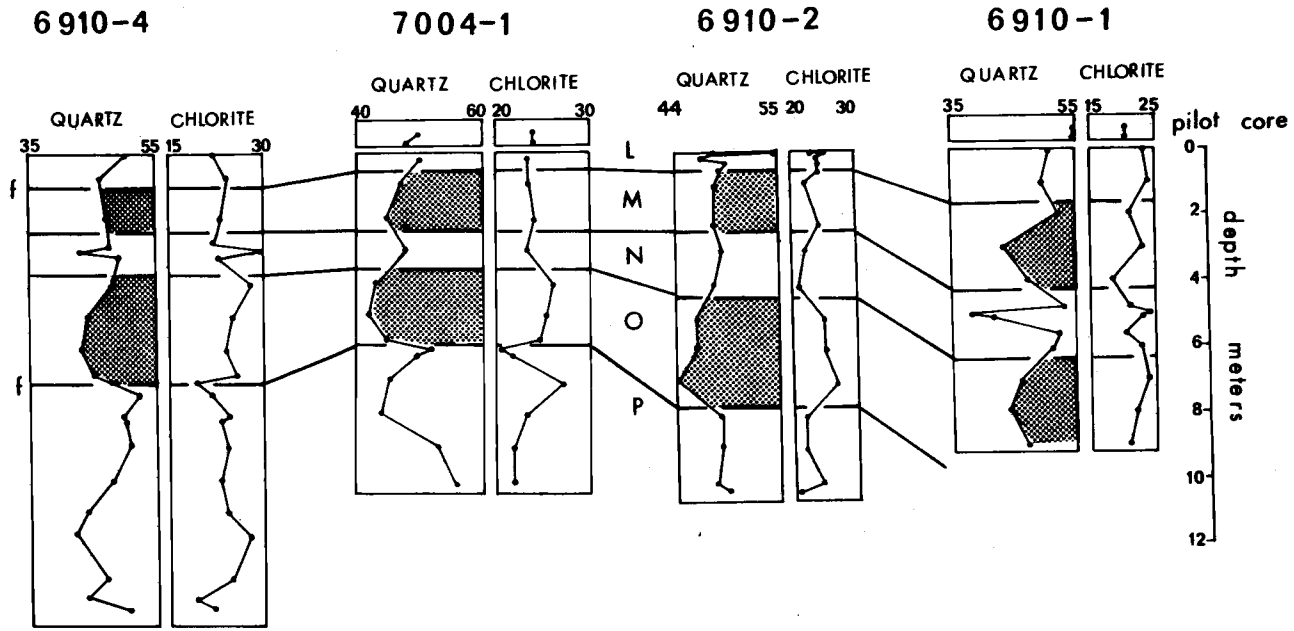

Figure 11. Comparison of mineralogical and microfossil datums in cores from the Gorda Ridge area. The letter "f" denotes the faunal datums. The numbers at the top of the cores are the percent concentration of the mineral.

formation were synchronous over the area studied.

Comparison of Mineral Datums and Late Quaternary Events

In any discussion of late Quaternary events it is instructive to compare the events of the area studied to those of a global nature. Figure 12 does this graphically. The zones rich in quartz, L, N, and P, coincide with periods of high solar radiation on the adjusted Milankovitch curve (Broecker, 1966, Figure 5); times of high sea level as shown by Veeh and Chappell (1970); and periods of catastrophic flooding in the Columbia River Basin as shown by Richmond et al. (1965). Zones low in quartz, M and O, were deposited during times of low solar radiation, and low sea level.

These correlations do not, in themselves, imply any cause and effect relationships. However, they do provide a constraint on the timing of processes that might effect the quartz abundance in the sediment.

Processes Effecting Quartz Abundance

There are three or four sedimentary processes that may account for the variations through time in the concentration of 2 to 20 micron quartz in the sediments of the Gorda Ridge area. These processes are related to changes in the eolian contribution, changes

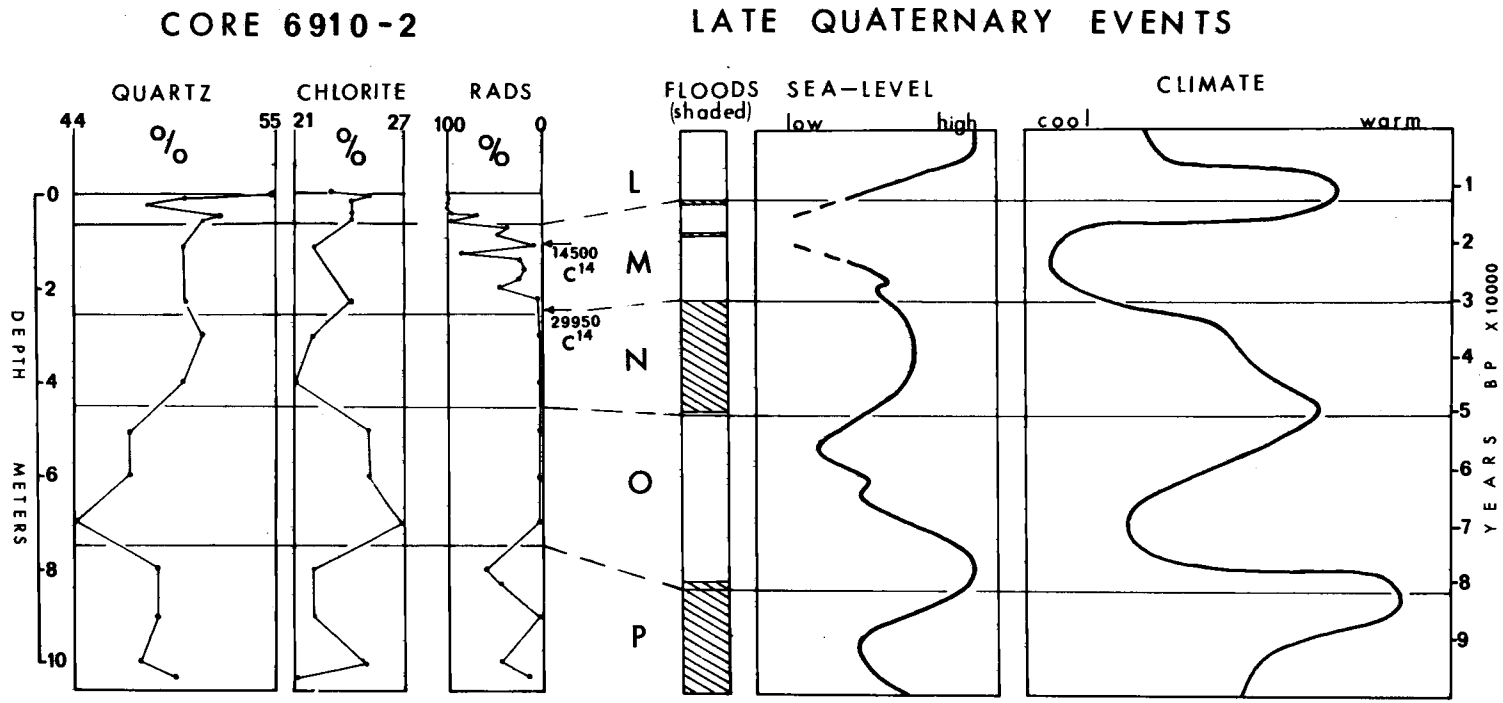

Figure 12. A comparison of mineralogic and micropaleontologic late Quaternary events. The data on floods are from Richmond et al. (1965); sea-level from Veeh et al. (1970); climate from Broecker (1966).

in sea level and catastrophic flooding of the Columbia River.

Eolian Contribution

Variations in the abundances of quartz in North Pacific deep-sea sediments have been attributed to changes in the eolian contribution to the sediments (Rex, 1958; Arrhenius, 1952, 1963). Windom (1969) suggests that as much as 75% of the total sediment of the central Pacific could be of eolian origin. These hypotheses apply to areas of low sedimentation rates (millimeters per 1,000 years).

The sedimentation rate on the Gorda Ridge area is roughly 10 cm/1,000 years, of which approximately 5.5 mm/1,000 years is quartz in the 2 to 20 micron fraction. Sedimentation rate data for quartz of this size, compiled from studies on atmospheric dust (Goldberg, 1971), snowfields (Windom, 1969) and deep-sea sediments (Rex, 1958; Opdyke and Foster, 1970; Griffin et al., 1968) range from 0.02 to 1.1 mm/1,000 years (Appendix 4). Using the maximum figure of 1.1 mm/1,000 years one can attribute about 20% of the quartz content of the Gorda Ridge sediment to eolian sources. Furthermore, if the sedimentation rate drops to 6 cm/1,000 years as it does in the upper part of core 6910-2, the eolian quartz amounts to 34% of the total quartz content of the sediment. If such a decrease in the total sedimentation rate were accompanied by an increase in the eolian contribution, the result would be a relatively

quartz-enriched sediment.

Rex and Goldberg (1958) suggest that the latitudinal variations in quartz they observed mirror fluxes in the troposphere and exposed areas of arid land that act as a source for the dust. They could not, however, determine which parameter was most significant. In this study the quartz-rich layers, L, N, and O, were deposited during times of high insolation (Figure 12). Such times would be marked by the existence of large areas of exposed glacial periods. Thus, the association of the quartz-rich zones with intervals of high insolation is consistent with the hypothesis that the quartz-rich sediment results from eolian quartz enrichment.

An analysis of Windom's (1969) data for dust collected on Mount Olympus shows that the 2-30 micron fraction has 25.8% quartz, 9.8% feldspar, 56% mica, 8.4% chlorite, and a trace of amphibole. These are the same minerals contained in a dust sample taken from the Gorda Ridge area (Figure 5) and the same minerals contained in the 2 to 20 micron fraction of the Gorda Ridge sediments, but the concentrations reported by Windom (1969) are considerably different. It is difficult to attribute a 40-50% quartz abundance in the sediment to accumulations of dust that contain only 26% quartz. The difference almost certainly results from the difficulty in comparing absolute and relative quartz concentrations discussed previously. Considering the nature of the available data on the present rate of supply of eolian

quartz (Appendix 3), it can only be suggested that the eolian contribution to the sediments of the Gorda Ridge area can partially account for the variations in the concentration of quartz deposited during the late Quaternary.

The Effects of High Sea Level

During times of high sea level much of the river sediment was trapped in the estuaries. Conversely, when sea level was low the rivers flowed across the shelf and injected their loads directly into the deep sea. Moore (1969) recognizes this effect in the turbidites of the California continental margin, as does Duncan (1968) in the sedimentation rates of the Cascadia Basin.

Thus, variations in sea level affect the rate at which sediments are being supplied to the deep sea. The effect on the quartz concentration in the sediment depends on the relative concentration of quartz in the various possible types of detritus. From the data for core 6908-5 (Table 1) it appears that the continental turbidites are quartz-poor relative to other sources (Duncan and Kulm, 1970; Rex and Goldberg, 1958). Thus, it seems that turbidites form a quartz-poor source of 2 to 20 micron quartz while eolian dust is relatively quartz-rich. During times of high sea level the turbidite contribution to the sediment was diminished and the sediments were enriched in eolian quartz. Dauphin (1972) made a detailed study of the particle

size distributions of 2 to 63 micron quartz separates from the upper part of core 6910-2. He concluded that the sediments in Zone L have a provenance different from that of the sediments in Zone M (Figure 12). It is logical to assume that at least part of this change in provenance can be attributed to eolian quartz enrichment during glacial times.

Catastrophic Floods

J. Harlen Bretz (1956, 1969), suggests that during the Quaternary, the Columbia River Basin was the site of a number of catastrophic floods resulting from the breaking of ice dams on the headwaters of the river. The huge volumes of water released eroded channels in the loess deposits of the Columbia River Basin. This picture has been substantiated by Richmond et al. (1965) who have constructed the chronology of flooding shown in Table 4. Note that each period of flooding is roughly coincident with a high quartz zone (Figure 12).

Such floods moved gravel down the Cascadia Channel as far as the Blanco Fracture Zone (Griggs et al., 1970) and must have carried enormous quantities of loess to the sea where much of it was deposited as pelagic sediment. An analysis of one of the loess deposits, the Palouse loess (Rieger and Smith, 1955) shows a grain size and mineral content very similar to that of the sediments of the

Table 4. Late Quaternary Columbia River floods due to ice dam failures (taken from Richmond et al., 1965).

FLOODS	AGE	GLACIAL NOMENCLATURE
Final flood on Columbia River	12,000 13,500	Everson Interstade Vashon Stade
Catastrophic flooding from 4 glacial lakes	? 18,000 ?	Recession Evans Creek Stade
Flood deposits from Lake Missoula	32,000 50,000	Late Stade, Salmon Springs or Bull Lake of The Rocky Mountains
Early flood of Lake Missoula	80,000 ? 100,000 ?	Stuck glaciation or Sacajawea Glaciation of the Rocky Mountains

Gorda Ridge. They report a size distribution of approximately 9% 50-100 microns, 66% 2-50 microns and 25% less than 2 microns. The large percentage of less than 2 micron material suggests that there is considerable 2 to 20 micron material available for deposition. Although there were no mineral analyses of the 2 to 20 micron fraction, their analysis of the coarser fraction shows it to be quartz-rich and contain feldspar, mica, and amphibole. Rex (1958) suggests that, on a global scale, loess averages about 50% quartz, a value which is compatible with the data of Rieger and Smith (1955).

Thus, the loess appears to contain enough 2 to 20 micron quartz to account for the changes in the mineral concentrations of the Gorda Ridge sediment. Furthermore, the inferred periods of maximum loess input to the deep-sea environment are coincident with the periods of deposition of the high quartz zones. For these reasons, it appears that deposition of loess resulting from catastrophic flooding in the Columbia River Basin is another factor affecting the composition of the sediment of the Gorda Ridge area.

CONCLUSIONS

Sediments on the higher areas of the Gorda Ridge are silty clays largely derived from the adjacent continent. An eolian component forms a minor but important part of these deposits. The silt fraction (2 to 20 microns) of these sediments consists of quartz, chlorite, mica and feldspar, as determined by X-ray diffraction methods. The determination of the relative abundances of each of these minerals reveal correlative stratigraphic changes in the silt size fraction. Using quartz as a key mineral, these changes can be related to variations in the late Quaternary climate.

Quartz-rich zones occur during periods of high solar radiation and high sea level (interglacial) while relatively quartz-poor zones occur during glacial times. These climatic changes caused variations in the eolian contribution to the sediment that were enhanced by changes in the sedimentation rates and deposition of flood sediment from the Columbia River. These variations account for the late Quaternary changes in the mineralogy of the sediments of the Gorda Ridge.

The coarse fraction of the sediment is dominated by radiolarian and foraminifera tests. Counts of these tests expressed as foraminiferan-radiolarian ratios confirm a change from a population dominated by radiolaria to one dominated by foraminifera at 12,500

years B. P. as noted by Duncan (1968). An older, previously unknown re-occurrence of radiolarian dominance occurs at about 83,000 years B. P. These changes in the Foraminiferal-radiolarian ratios bracket the mineralogical variations found in the cores, and confirm the independently derived correlation of quartz datums.

The clay fraction (<2 micron) of the sediment is composed of smectite, illite and chlorite. Cores taken from topographic highs on the Gorda-Juan de Fuca plate contain less smectite than cores from nearby turbidites. This relation is consistent with the idea that these sediments are enriched in eolian detritus because dust samples collected from the continent also have an extremely low smectite contents.

PART II: TECTONICS

INTRODUCTION

Numerous authors (Atwater, 1970; Silver, 1971b; Morgan, 1968) have referred to the Gorda plate while others talk of the Juan de Fuca plate. Clearly there is no evidence that these have ever existed as separate lithospheric plates, and a comment on nomenclature is needed at this point. The terms Gorda plate and Juan de Fuca plate have generally been used in a geographical context rather than a geophysical one. To preserve this most useful geographical distinction and not abuse the obvious geophysical implications of the term "plate," the two entities will be referred to as sub-plates in this discussion. Thus, the Gorda-Juan de Fuca lithospheric plate is composed of the Gorda sub-plate and the Juan de Fuca sub-plate and each sub-plate is discussed as a separate entity.

The physiographic features of the northeast Pacific sea floor are well known (Figures 1 and 2). The origins of these features have recently been described in terms of plate tectonics. For example, the pattern of magnetic anomalies described by Mason and Raff (1961) have been explained by Vine (1966) as representing periods of reversals in polarity of the earth's magnetic field recorded in the rocks of the sea floor. Another example is Wilson's (1965) development of the concept of transform faulting to explain the Mendocino

and Blanco Fracture Zones. Such explanations of the geometry and magnetic lineations of the sea floor were incorporated into the plate tectonic hypothesis by Morgan (1968). He described sea floor features in terms of moving rigid lithospheric plates. Yet the magnetic anomaly pattern of the northeast Pacific would not fit such an explanation and was specifically deleted from consideration by Morgan (1968) because the plates of the area were not acting like rigid bodies, but were deforming internally. Several other authors, including Isacks, Oliver and Sykes (1968); Atwater and Menard (1970); Atwater (1971); and Silver (1971a) have restated this assertion. Specifically these workers suggest that the Gorda and Juan de Fuca sub-plates are not rigid lithospheric sub-plates, but are undergoing internal deformation. The seismicity studies of Tobin and Sykes (1968) and Seeber et al. (1970) have produced some insight into the deforming forces on the Gorda sub-plate. Seeber et al. (1970) conclude that the Gorda sub-plate is a region of crustal shortening caused by regional (north-south) horizontal compression. Finally, Dehlinger et al. (1967) identified a low density block beneath the Mendocino Fracture Zone which (Silver, 1971a) may correspond to the underthrust Gorda sub-plate. The underthrusting could be the result of the stresses described by Seeber et al. (1970). It is apparent, then, that any historical reconstruction of the Gorda and Juan de Fuca sub-plates must consider the plate deformation and concurrent plate growth. It

is the purpose of this paper to consider such a reconstruction.

Some of the earlier models of deformation of the sub-plate called upon events that were not substantiated by later geophysical work. Two such instances of this are, the suggestion of Pavoni (1966) that large portions of the Juan de Fuca sub-plate have been destroyed, and the suggestion of Peter and Lattimore (1969) that the rotation of the Juan de Fuca sub-plate resulted from strike slip faulting. In other cases the interpretations of sub-plate deformation have been vague or ambiguous. For example, the 15 to 20° change in the orientation of the anomalies generated at the Juan de Fuca Ridge was interpreted by Menard and Atwater (1968) as the result in global changes in the sea floor spreading pattern. Similarly, Morgan's (1968a) attempt at a Pliocene reconstruction of the area resulted in no unique solution to the development of the plates. A much better reconstruction of the area is possible at this time because of the general development of plate tectonic theory and the availability of continuous seismic profiles in the area, neither of which was available to these earlier workers.

This paper suggests a model or hypothesis of deformation of the Gorda and Juan de Fuca sub-plates that is consistent with the late Cenozoic Pacific plate movement described by Atwater (1970) rather than the model described by Pitman and Hayes (1968). The interpretations of the magnetic anomaly pattern presented by Vine

(1968) are the primary data for the hypothesis, although the magnetic anomaly interpretations of Melson (1970), Peter and Dewald (1971) and Atwater and Menard (1970) are also used. Continuous seismic profiles taken in conjunction with this study at Oregon State University, as well as published profiles from Ewing et al. (1968), Silver (1970) and Carson (1971, 1973), have been used to describe the sediment plate interaction.

The hypothesis was tested by attempting to generate the present anomaly configuration as shown in Figure 13 (Vine, 1968) from earlier configurations. The earlier magnetic anomaly configuration on the Juan de Fuca Ridge area was constructed in the following fashion. Anomalies from the east side of the Juan de Fuca Ridge were first restored to their original lengths (Figure 14) by removing the effects of the faulting. The positive anomalies were then cut out of Figure 14 with a scissors and the resulting strips of paper duplicated to represent the western Pacific plate anomaly halves. The result is shown in Figure 15. A further constraint was that all of the anomalies were cut off at the 47th parallel, thus the deformation occurring at the northern end of the Juan de Fuca sub-plate is not considered. The Gorda Ridge area was treated in a similar fashion, except that the anomalies from the western side of the ridge were cut out with a scissors and duplicated to form the original undeformed Gorda plate as shown in Figure 16.

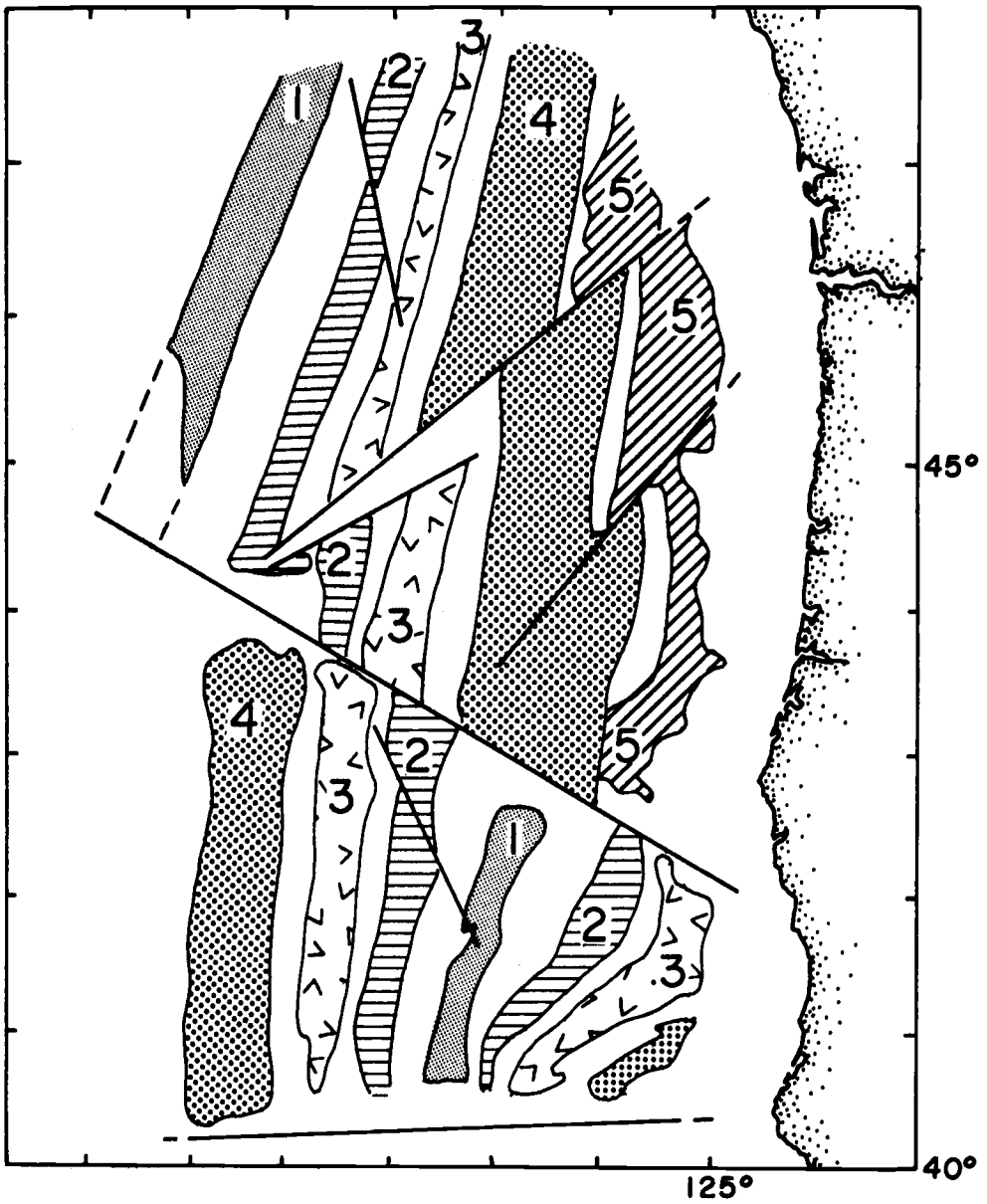

Figure 13. The present geometry of the magnetic anomalies on the Gorda and Juan de Fuca plates. Taken from Vine (1968).

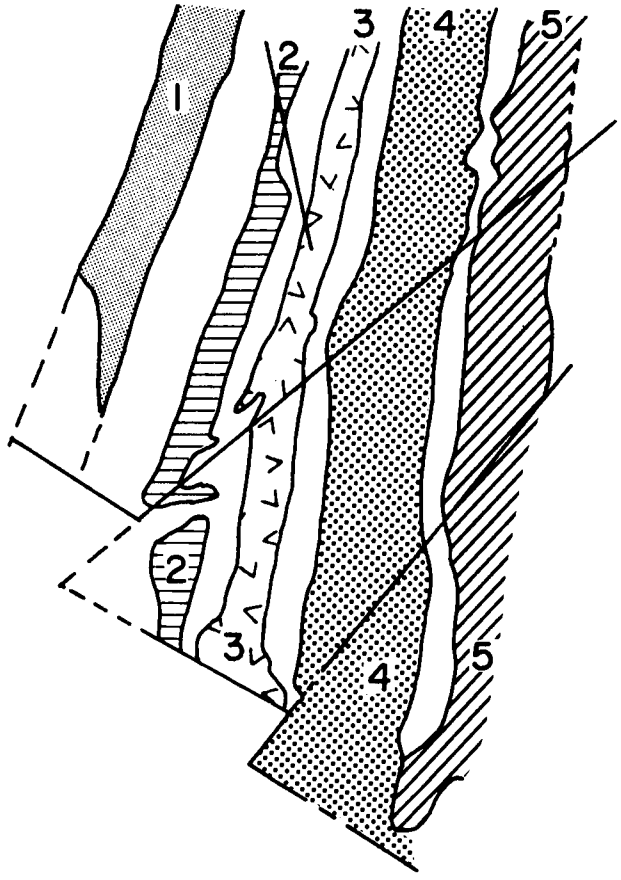

Figure 14. The anomalies of the Juan de Fuca plate after the effects of the faulting have been removed. This figure was constructed directly from Figure 13. Note that the plate is longer (N-S) and thinner (E-W) than it is in Figure 13.

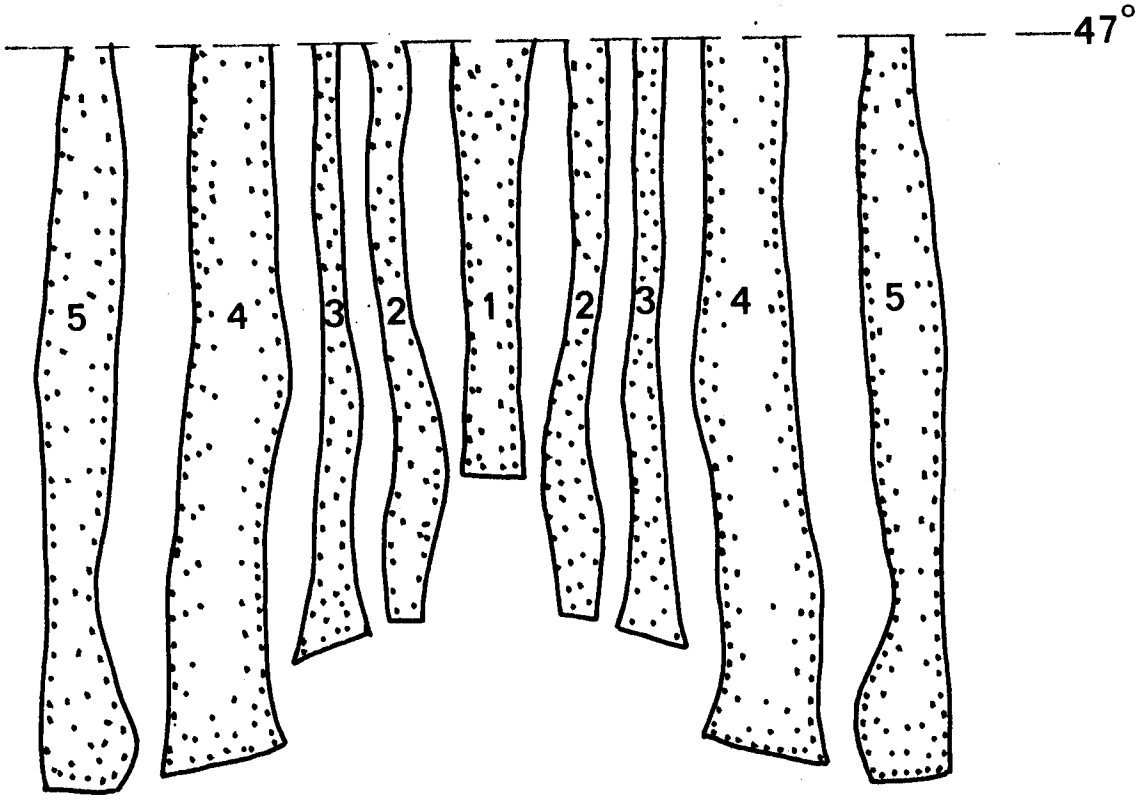

Figure 15. A reconstruction of the anomalies generated at the Juan de Fuca Ridge. The figure was constructed using the anomaly pattern from Figure 14 and duplicating it to fabricate the anomalies on the Pacific plate. All the anomalies are "hung" on the 47th parallel to show the shortening, in pairs, of each anomaly.

Using these anomaly strips from the two ridges, the sub-plates were reconstructed from anomaly four time (7.4 million years B.P.) to the present by sequential addition of anomaly halves. These reconstructions were made on a xerox copier so that each step could be recorded. Multiple reconstructions were made until one was developed that would generate the present magnetic anomaly pattern using what seemed to be reasonable assumptions.

These assumptions were:

1. Anomalies are generated at the ridge crest and they reflect the length of the ridge at the time they were generated.
2. The Gorda-Juan de Fuca plate has been subducted at the North American plate boundary.
3. Transform faulting is occurring at the Blanco Fracture Zone and the Mendocino Fracture Zone.

The reconstructions require a shortening of the anomalies of the Juan de Fuca Ridge as well as those of the Gorda Ridge since anomaly five time, approximately 10 million years ago. Furthermore, it is proposed that the shortening of the Gorda sub-plate by overthrusting of the Pacific plate and the shortening of the Juan de Fuca sub-plate by the two episodes of shear faulting that occurred in Cascadia Basin were major factors in the development of the present configuration of these plates.

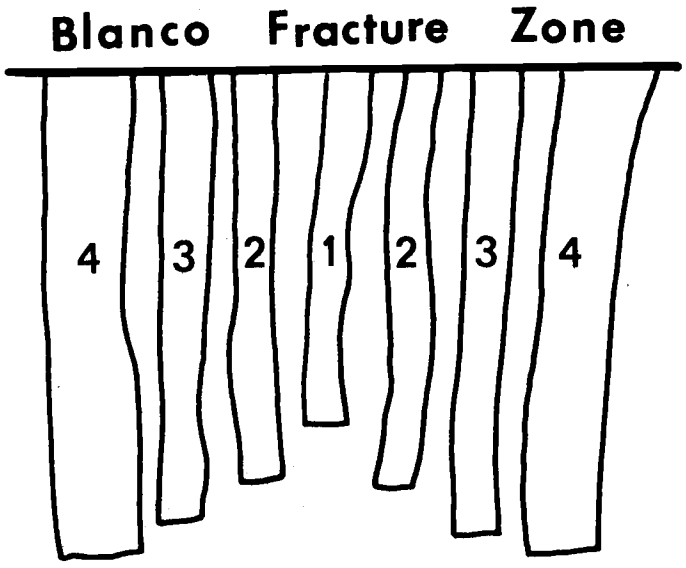

Figure 16. The anomalies generated at the Gorda Ridge. This figure is derived from Figure 13, by duplicating the positive anomalies from the left (Pacific plate) side of the central anomaly and placing them on the right. The anomalies are aligned along the Blanco Fracture Zone to show their continuous shortening.

DEFORMATION OF THE GORDA SUB-PLATE

The anomalies of the Gorda sub-plate were reconstructed to show the sub-plate as it would appear with no relative movement between it and the Pacific plate, and no deformation except that which shortened the anomalies. To do this, the undeformed anomalies from the west side of the ridge were duplicated and aligned along a hypothetical Blanco Fracture Zone (Figure 16).

It is proposed, as a working hypothesis, that the decrease in the length of the anomalies five through one occurred as a result of the continental overthrusting of the Pacific plate at the Mendocino Fracture Zone. If this overthrusting is the dominant shortening process, the anomalies show that it has occurred continuously for the last 10 million years, since the formation of anomaly five. Prior to that time, the anomalies are unclear and the interpretations questionable (Atwater and Menard, 1970).

If the Pacific plate portion of the Gorda Ridge anomalies moved northward and the Gorda sub-plate anomalies did not, it is easy to develop the anomaly pattern as it appears today. Figure 17 shows the proposed sequence of events leading to the present configuration of magnetic anomalies. The relative non-spreading motion between the Pacific and Gorda plates is one of dextral strike slip along the ridge itself. Tobin and Sykes (1968) note the possibility of such a

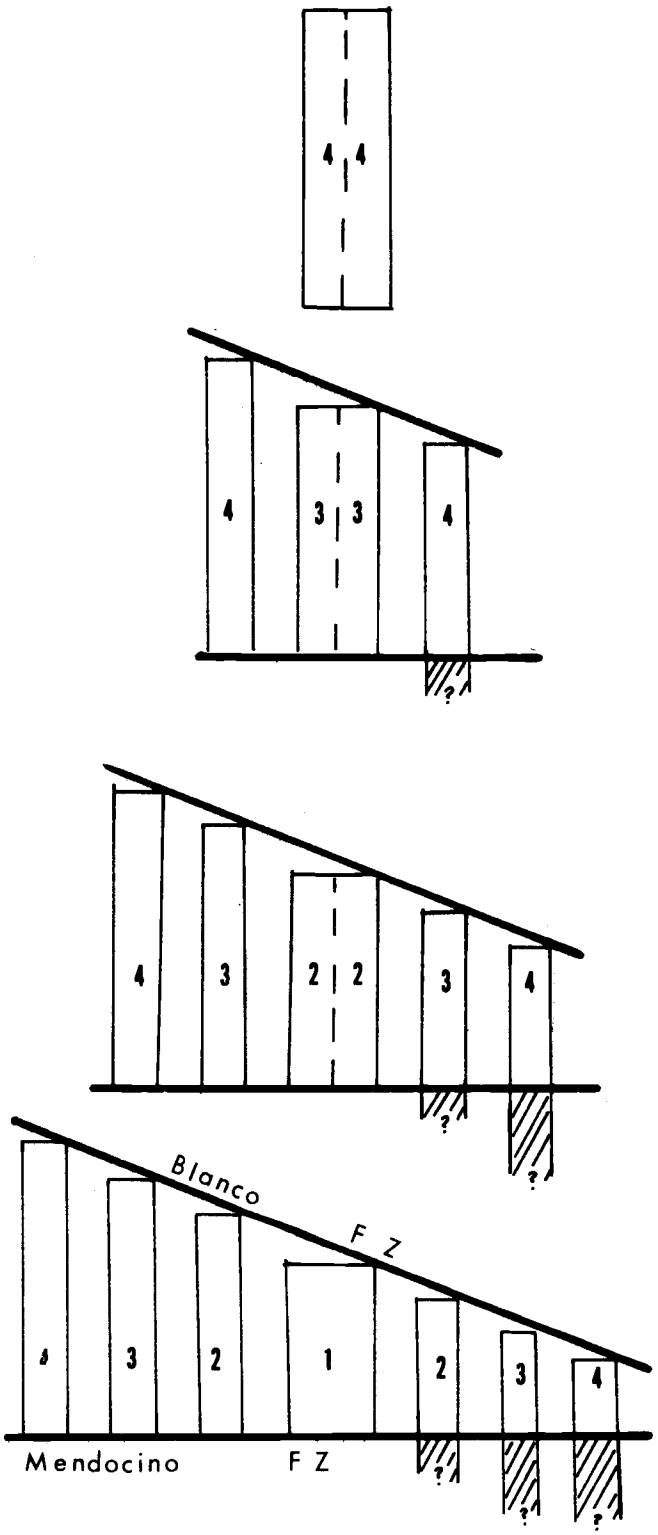

Figure 17. A diagrammatic portrayal of the development of the Gorda sub-plate. The western half of each anomaly moves northward with the Pacific plate, while the eastern halves of each anomaly are shortened by overthrusting of the same Pacific plate. The overthrust portions of each anomaly are shaded.

movement in their first motion seismic studies. Less direct evidence of such relative motion between the two plates is explored later in this paper.

Such a model of the deformation of the Gorda sub-plate has several consequences. First, it suggests that the older anomalies of the Gorda sub-plate should be more deeply underthrust than the younger anomalies. This is consistent with the work of Dehlinger et al. (1967) who show the low density blocks under the Mendocino escarpment to be deepest on the profiles nearest the continent, that is below the older anomalies (Figure 18). These older anomalies are also more highly deformed than their younger counterparts, having been twisted out of their northwest-southeast orientation by the movement of the Pacific plate along the Mendocino Fracture Zone.

A second consequence of the proposed model of Gorda sub-plate deformation is that the Blanco Fracture Zone, which is the boundary between the Pacific plate and the Juan de Fuca sub-plate, must be rotated out of its normal perpendicular relationship with the bounding ridges to conform to the progressively shortened anomalies that abut it (Figure 19). This oblique relationship of the Blanco Fracture Zone to the Gorda and Juan de Fuca Ridges have been interpreted by other authors as the result of a regional change in spreading direction (Pitman and Hayes, 1968; Menard and Atwater, 1968), or as an attempt to align the Blanco Fracture Zone with the San Andreas

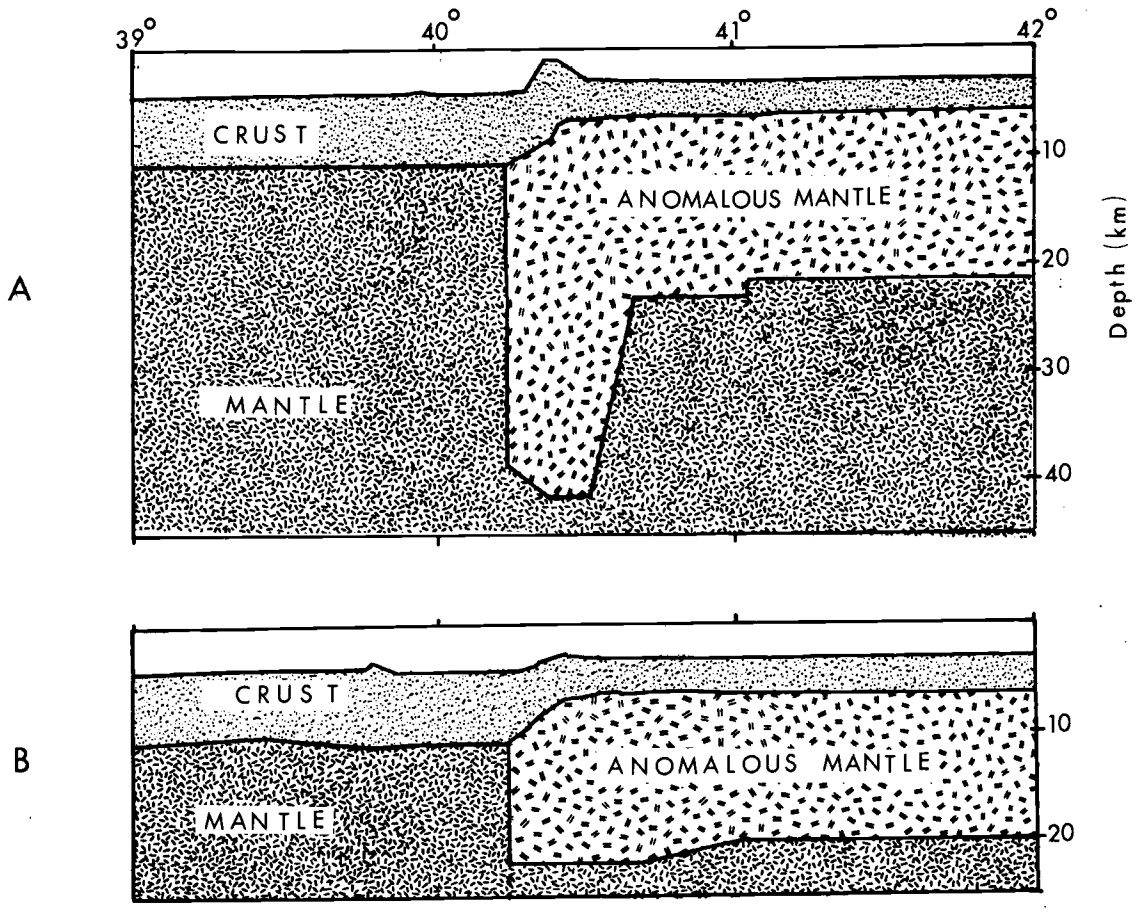

Figure 18. Crust and subcrustal cross-sections across the Mendocino Fracture Zone after Dehlinger et al. (1968). Section A is along 127°30' West longitude and Section B is along 128°20' West longitude.

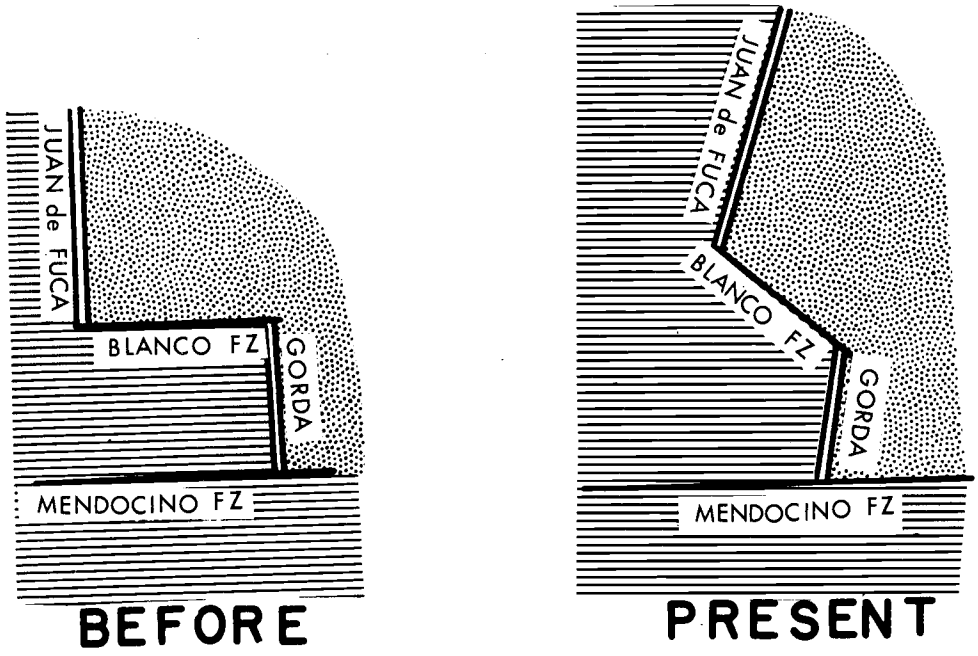

Figure 19. Changes in the configuration of the Blanco Fracture Zone.

trend (Seeber et al., 1970). The hypothesis presented here is that the oblique position of the Blanco Fracture Zone is a consequence of progressive shortening of anomalies generated along the Gorda Ridge due to northward movement of the Pacific plate and simultaneous underthrusting of the Mendocino Fracture Zone as shown in Figure 17.

Another consequence of the progressive shortening of anomalies generated along the Gorda Ridge is the rotation of the Juan de Fuca plate. Menard and Atwater (1968) note that magnetic anomalies four through three on the Pacific plate just west of the present Juan de Fuca Ridge record a change in trend from north-south in anomaly four time to northeast-southwest by anomaly three time. Such a rotation is the response expected of the Juan de Fuca sub-plate as it moved against the progressively shortened Pacific plate anomalies. It may be presumptuous to conclude that the shortening of the Gorda Ridge anomalies ultimately caused the rotation of the Juan de Fuca sub-plate to its present northeast-southwest orientation, but such a rotation is certainly required by the geometry of the two plates when considered within the framework of the proposed model.

DEFORMATION OF THE JUAN DE FUCA SUB-PLATE

If the anomalies of the Juan de Fuca sub-plate are restored to their original length by removing the left-lateral shear faults, they

are lengthened as has been noted by Pavoni (1966) and Silver (1971), (Figures 13 and 14). If these longer anomalies are duplicated to represent the Pacific plate portion of the anomalies generated at the Juan de Fuca Ridge, the result is a pattern displayed in Figure 15. This pattern would also represent the anomaly configuration if there were no relative movement between the Pacific plate and Juan de Fuca sub-plate.

As was the case with the Gorda Ridge, a series of progressively shortened anomalies implies a decreasing ridge length. Unlike the Gorda Ridge situation, the anomalies of the Juan de Fuca Ridge appear to shorten in pairs. Anomalies four and five are about the same length as are anomalies two and three. On the eastern side of the ridge, each pair is offset by a large left-lateral shear fault. Silver (1971) suggests that the plate is shortened by the faulting and this concept is incorporated into the present working hypothesis that the shortening of the anomalies and the faulting show a cause and effect relationship. Each fault shortened the plate considerably. Thus, the anomalies formed prior to the faulting are longer than those that were formed after the faulting. For example, anomalies four and five are longer than anomalies two and three. The anomalies of the Juan de Fuca sub-plate show two episodes of faulting that resulted in two stages of shortening.

The Effects of Plate Movement

Figure 20 shows how the present magnetic anomaly pattern on the Pacific plate adjacent to the Juan de Fuca Ridge was developed. The northerly motion of the Pacific plate relative to the Juan de Fuca sub-plate has offset the magnetic anomalies northward. A similar configuration of Pacific plate anomalies is shown on the map of Atwater and Menard (1970, Figure 1, page 446). It is interesting to note that the Pacific plate extension of the Blanco Fracture Zone should also be bent to the northwest by such plate motion. Peter and DeWald (1971) report the discovery of a fracture zone trending obliquely northwest from the junction of the Juan de Fuca Ridge and the Blanco Fracture Zone. They suggest that the fracture zone originated as a result of some late Tertiary deformation of the entire area, rather than simply an oblique extension of the Blanco Fracture Zone as proposed here.

The northerly motion of the Pacific plate is considered as the primary cause of shortening of the Gorda and Juan de Fuca sub-plates as was mentioned above. If this consideration is valid then the Gorda and Juan de Fuca sub-plates cannot be moving with the Pacific plate but must be lagging behind. This was suggested by Atwater (1971) while a vector analysis of the plate motions led Silver (1971) to a similar conclusion. The examination of the shortening that has

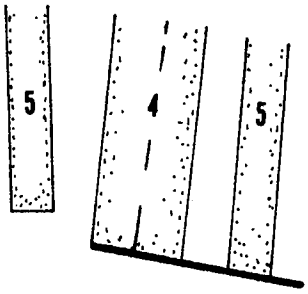

A. Anomaly 4 time. The Pacific plate anomaly 5 has moved northward. The Blanco Fracture Zone has already tilted southeast.

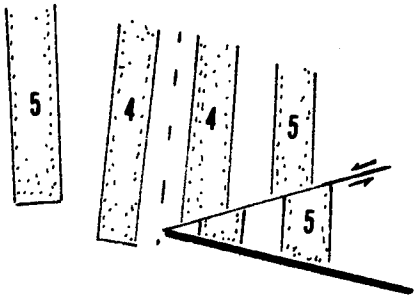

B. After the implacement of anomaly 4, shear faulting shortens the plate. Anomaly 4 on the Pacific plate is left hanging below the Blanco Fracture Zone.

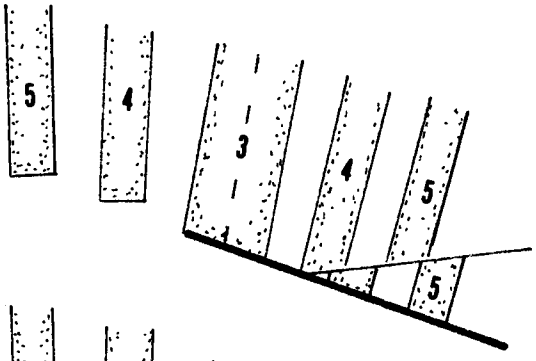

C. A shorter anomaly 3 is implaced while the eastern anomalies 4 and 5 move northward with the Pacific plate.

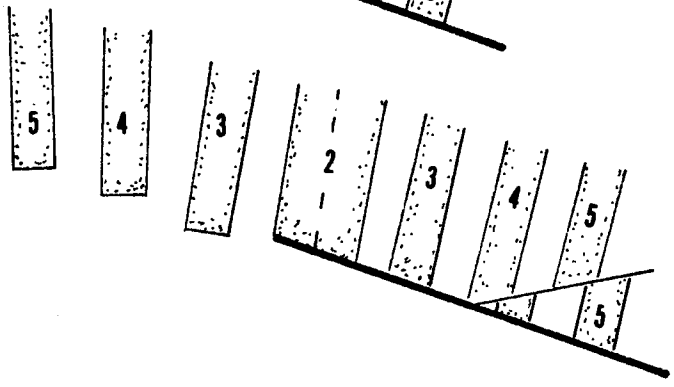

D. Anomaly 2 is implaced. It is the same length as anomaly 3.

Figure 20. The development of the Juan de Fuca sub-plate from anomaly 4 time to the present. The spreading motion of the ridge; the northerly movement of the Pacific plate; and the shortening of the Juan de Fuca sub-plate by shear faulting are key factors in the plate's history.

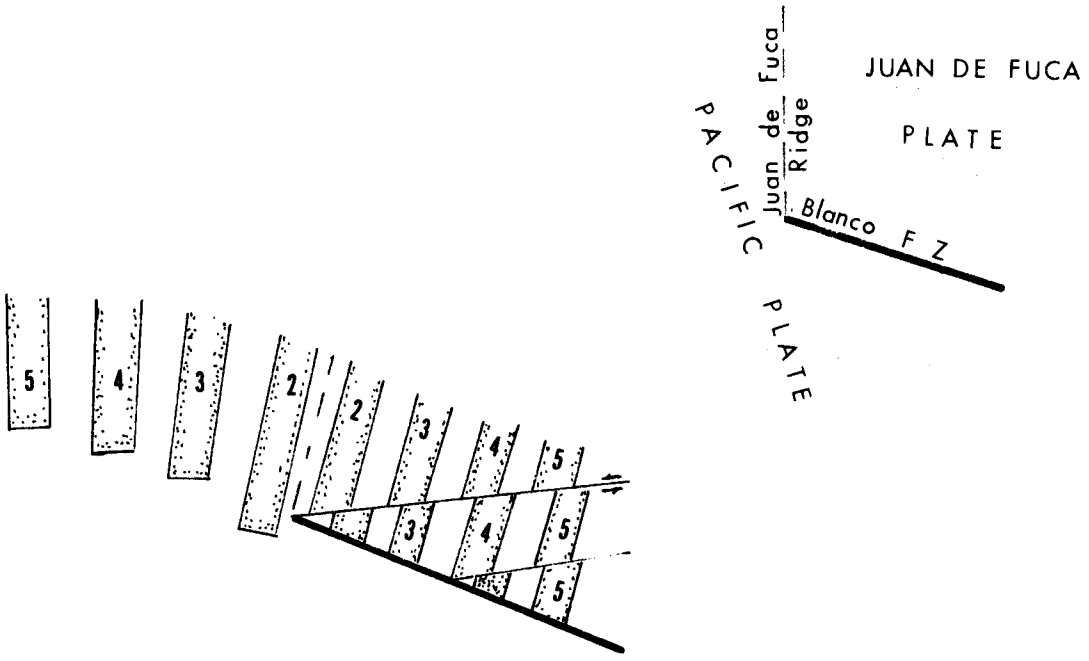

E. After anomaly 2 is implaced, a second episode of shear faulting again shortens the plate, leaving anomaly 2 hanging below the present Blanco Fracture Zone.

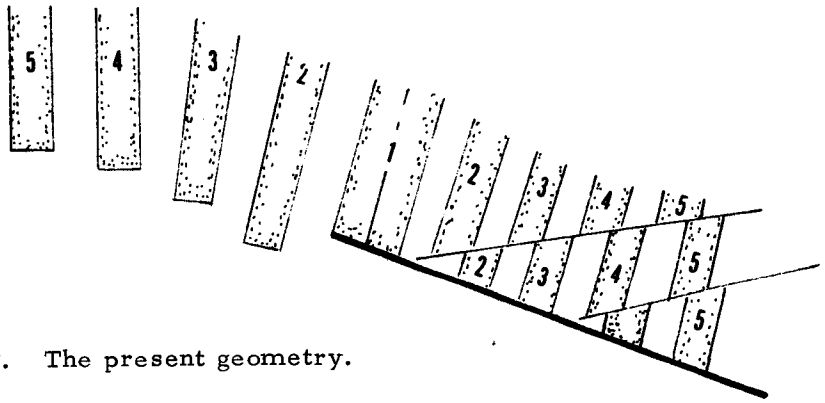

F. The present geometry.

Figure 20. Continued.

occurred since anomaly four time (approximately 7.4×10^6 yrs. B.P.) strengthens the conclusions of these two authors. A comparison of the present length of anomaly four as it is found on the Gorda and Juan de Fuca sub-plates (Figure 13) with it original lengths shows it to be several hundred kilometers shorter. In particular, a restoration of the faulting on the Juan de Fuca sub-plate shows a shortening of approximately 90 kilometers while a comparison of the lengths of anomaly four on the west side of the Gorda Ridge with the entire east side of the Gorda sub-plate (most of anomaly four has been subducted) shows a shortening of approximately 210 kilometers. Thus, the combined shortening for these two plates is about 300 kilometers in 7.4×10^6 yrs. or approximately 4 cm/yr.

These suppositions require right lateral strike slip movement along the Gorda and Juan de Fuca Ridge crests. One might look to seismic data for some confirmation of such movement but the results are discouraging. There is little seismic data available on the Juan de Fuca Ridge crest due to its low seismicity and most of the available data on the Gorda Ridge has been interpreted as dip slip faults (Tobin and Sykes, 1968; McEvilly, 1968). There is one questionable event reported by Tobin and Sykes (1968, event 2, page 3838) on the northern end of Gorda Ridge that suggests right lateral strike slip movement. Thus, while there is good long-term evidence (7 million years) to suggest that the Gorda and Juan de Fuca sub-plates

are not moving with the Pacific plate, there is little short term support (last 10 years) to confirm such movement.

Another area where shorter term deformations appear to differ from long term trends lies just west of the intersection of the Juan de Fuca Ridge and the Blanco Fracture Zone. Here an intensive survey by Melson (1969) provides data that suggest that the Juan de Fuca sub-plate deformed abruptly leaving some of the Pacific plate anomalies extending south of the present ridge-fracture zone intersection (Figure 21). More specifically, the data from Melson's (1969) survey suggest that left lateral shear faulting shortened the Juan de Fuca sub-plate (and ridges) sometime after the Jaramillo event, leaving the Pacific plate, Jaramillo and Gaussian anomalies extending below a westward projection of the Blanco Fracture Zone. The conclusion is that the rate of shortening of the Juan de Fuca sub-plate due to the faulting was considerably greater than the northerly motion of the Pacific plate, creating the apparently anomalous situation.

The Regional Acoustic Disconformity in Cascadia Basin

The shear faulting that offsets the anomalies in the Juan de Fuca sub-plate effectively shortened the sub-plate in a north-south direction (Pavoni, 1966) and widened it in an east-west direction (Silver, 1971). One of the effects of widening the sub-plate would be to

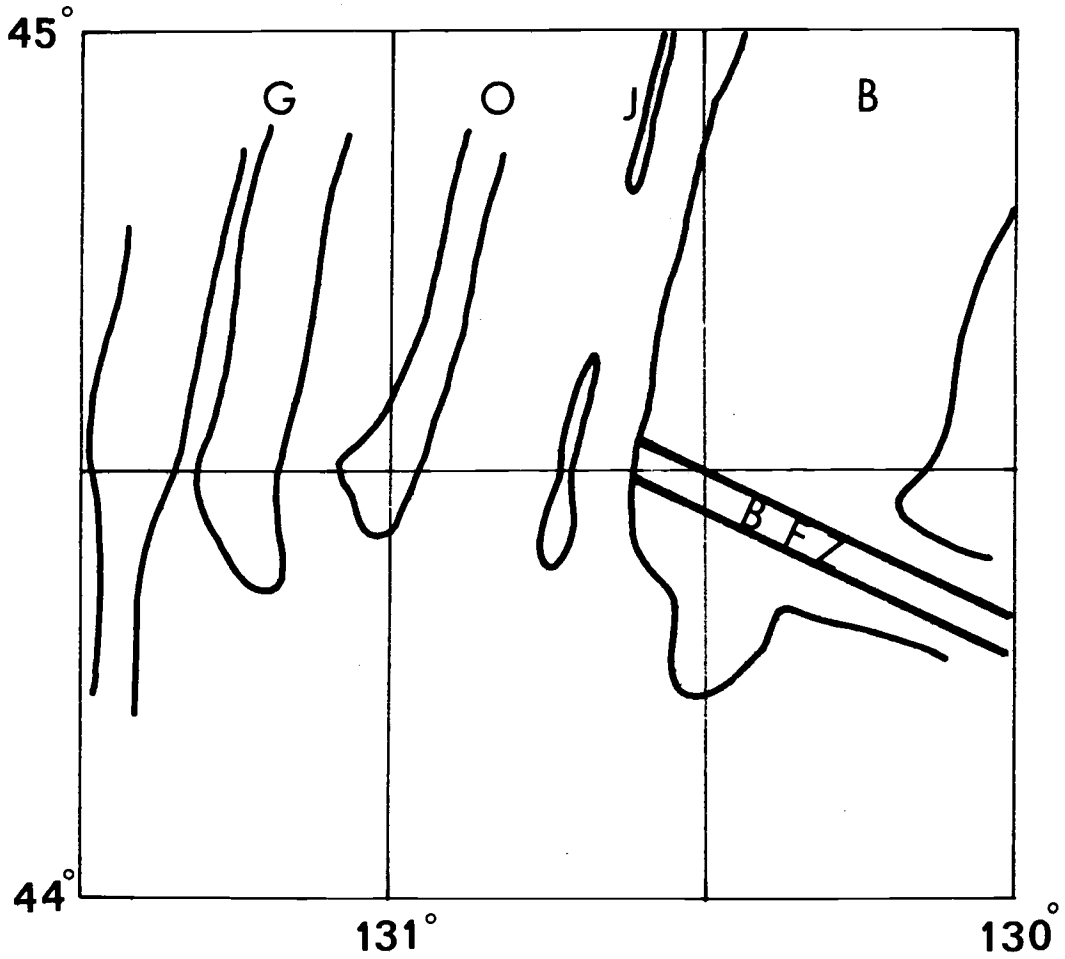

Figure 21. A detailed map of the magnetic anomalies west of the Blanco Fracture Zone. The Gauss (G), Olduvai (O), and Jaramillo (J) anomalies extend below the present extension of the Blanco Fracture Zone, suggesting that the Juan de Fuca Ridge has been shortened after they formed.

increase the rate of subduction (pointed out by Silver, 1971). The sediments on the eastern side of the Juan de Fuca sub-plate and on the adjacent continental margin record the effects of this rapid subduction.

Continuous seismic profiling near the margin of the continent show that the basement and some of the overlying sediments plunge beneath the turbidites of the Astoria Fan to form a disconformity (Figure 22). This disconformable relationship can be recognized in Profiles C, G, and H (Figure 23), as well as in the profiles published by Ewing et al. (1968) and Carson (1973). The disconformity appears to be a regional feature associated with the entire eastern side of the Cascadia Basin. It does not appear in the profiles published by Silver (1969) on the eastern side of the Gorda plate. Thus, the acoustic disconformity seems to be associated only with the Juan de Fuca sub-plate, which is to be expected if it formed as the result of faulting on that sub-plate.

Hole 174 of the Deep Sea Drilling Project, Leg 18 (Kulm, von Huene et al., 1973), penetrated the acoustic disconformity (Figure 24). They describe a turbidite section consisting of two major units, an upper unit (0-284 meters) consisting of upper Pleistocene medium to very fine turbidite sands and a lower unit (284-879 meters) consisting of upper-lower Pleistocene and Pliocene thin bedded fissle silty clays with graded basal silt intervals. Concerning the

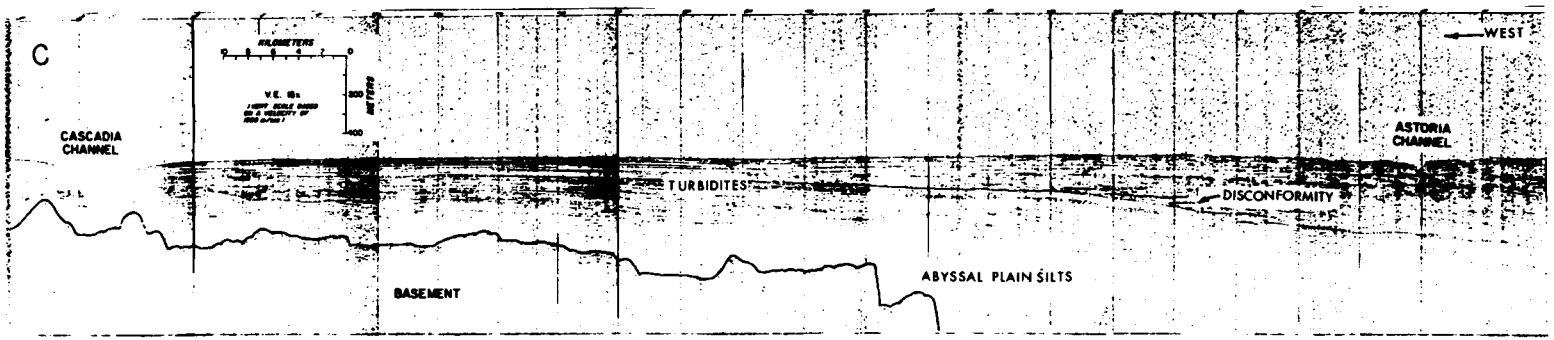

Figure 22. A retouched photo of a continuous seismic reflection profile showing the acoustic discontinuity.

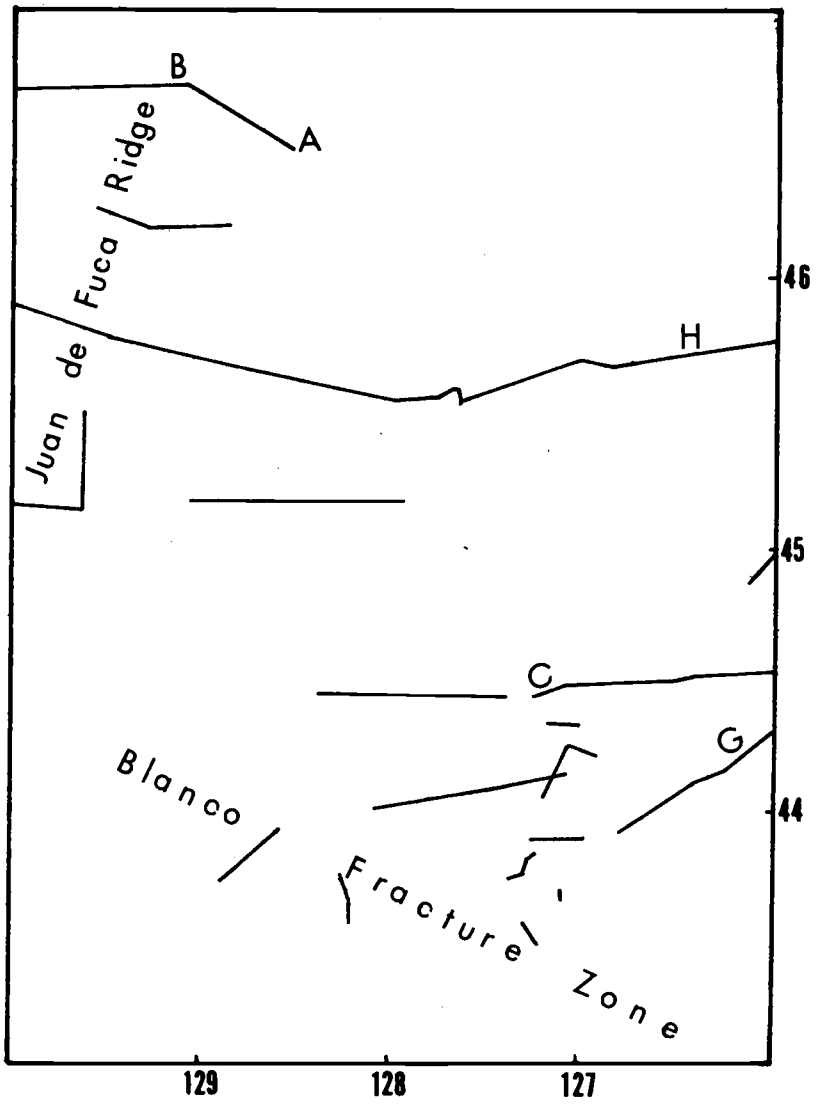

Figure 23. Continuous seismic profiles of the Cascadia Basin, made by Oregon State University.

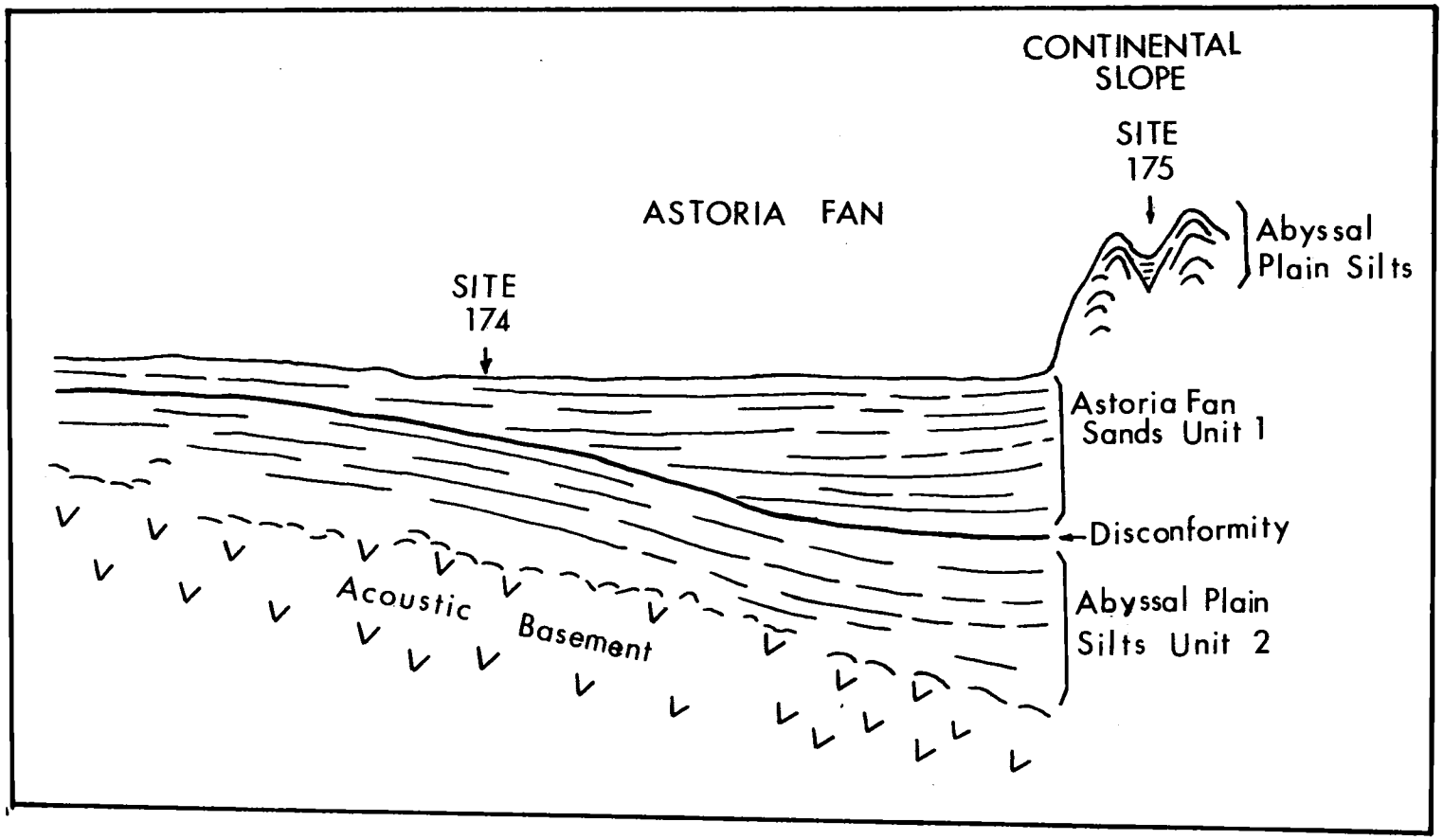

Figure 24. Location of the Deep Sea Drilling Project Site 174 relative to the discontinuity and the continental margin.

acoustic disontinuity, they (Kulm, vone Huene et al., 1973, page 102) state: "The acoustic disontinuity noted on the seismic reflection records corresponds approximately to the break between the two major lithologic units. There is no indication, based upon the fauna, flora and lithologies, that the discontinuity is an erosional surface or represents a major break in the depositional record. The glacial and interglacial intervals occur above and below it suggesting that this surface is not solely the result of increased sedimentation rates associated with the glacial Pleistocene."

The formation of a disconformity without a major break in the depositional record can be accomplished by sedimentation on a moving plate as shown in Figure 25. The increased subduction rate due to the shear faulting carried the sediments of Unit 2 that were deposited out on the Cascadia Abyssal Plain back down into the subduction zone. These down-bent sediments were onlapped by younger turbidite (Unit 1), resulting in the formation of the disconformity. Thus, the formation of the acoustic discontinuity can be directly related to tectonism in the Cascadia Basin.

Time of Faulting

The relationship between the acoustic disontinuity and the shear faulting can be tested by checking their synchroneity. Kulm, von Huene et al. (1973, page 965) suggest an upper Pleistocene age for the

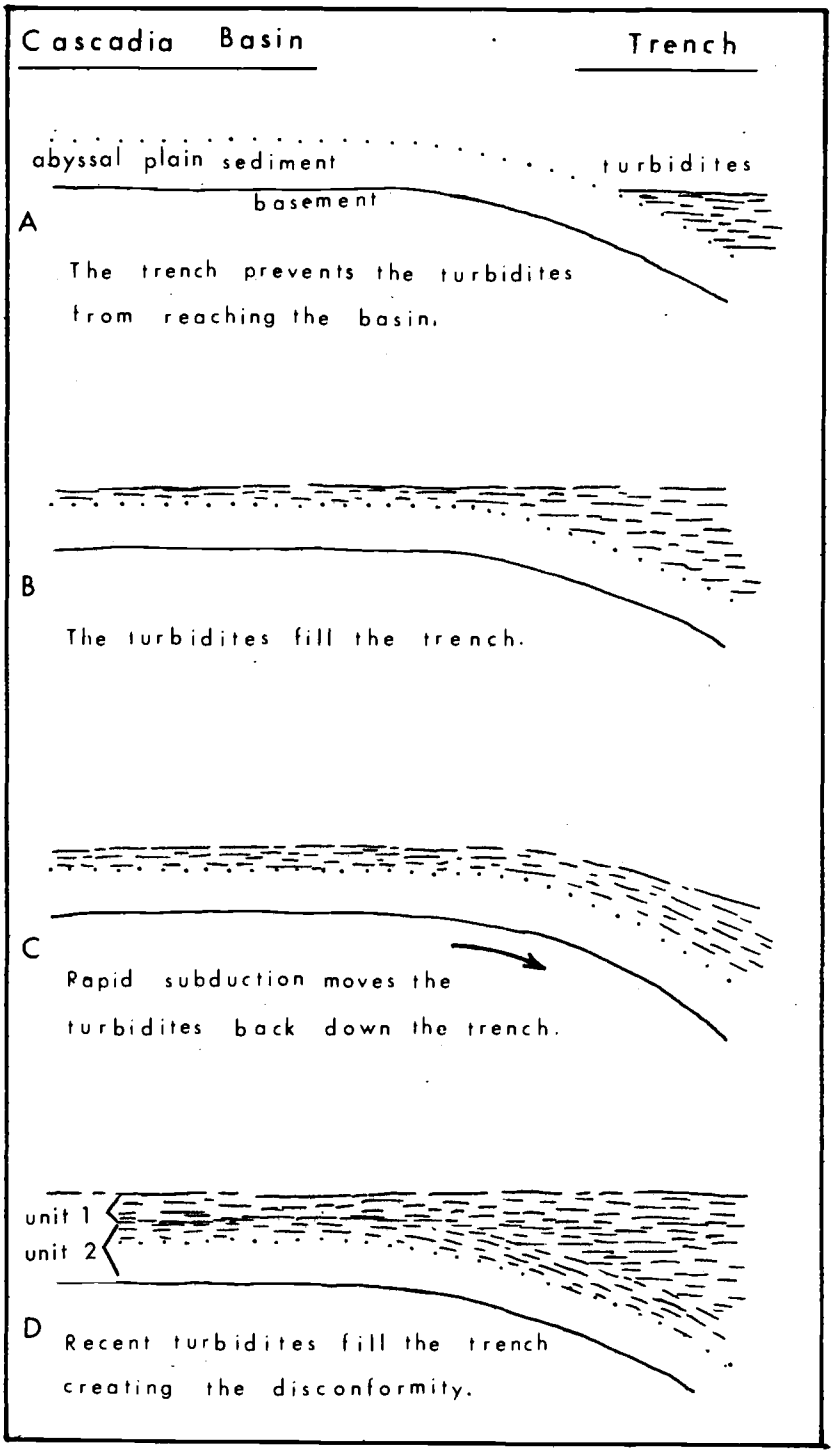

Figure 25. Steps in the formation of the discontinuity at the eastern edge of the Cascadia Basin. The dotted line in the lower part of Unit 2 represents the change in heavy mineral suites and provenances of the sediments as reported by Kulm, von Huene et al. (1973).

discontinuity corresponding to an age that is younger than 1.0 to 1.2 million years. Using the geomagnetic data presented by Melson (1969) in the context of the hypothesis proposed in this paper, the youngest fault is post-Jaramillo (approximately 10^6 years) in age. Thus, the age of the youngest faulting falls within the range of the proposed age of the acoustic discontinuity and the two events can be considered to be approximately synchronous.

There may be a record of this younger shear faulting left in the sediments of the continental margin. Assuming that the folds of the sediments of the continental margin are formed through a subduction process as proposed by Silver (1969, 1972) and Kulm, von Huene et al. (1973) then times of rapid subduction should correspond to periods of increased deformation. Von Huene et al. (1971) suggest that a middle to late Pleistocene period of folding and uplift is coeval with a Pleistocene unconformity penetrated in Hole 176 during Leg 18 of the Deep Sea Drilling Project. Von Huene and Kulm (1973, page 965) report that the age of this unconformity is possibly one million years or younger. This falls with the age range of the youngest shear fault and the acoustic disconformity. There is another unconformity of a regional nature on the Oregon continental margin that has been dated as middle to late Miocene (Kulm and Fowler, 1971; Kulm and Fowler, in press). This older unconformity may well have resulted from accelerated subduction that occurred during the older period of

shear faulting, which is tentatively dated on the basis of the magnetic anomalies as approximately 7 million years old. Thus, there are two unconformities in the sediments of the continental margin whose ages roughly correspond to the ages of the shear faults.

The Blanco Fracture Zone

One of the necessary corollaries of the working hypothesis is that the Blanco Fracture Zone has maintained its general orientation for some time. This is contrary to the suggestions of Atwater (1970), Melson (1968), and Peter and DeWald (1971), who favor a recent change in the orientation of the Blanco Fracture Zone. However, because the Pacific plate side of the Blanco Fracture Zone is not perpendicular to the adjacent ridges due to shortening of the Gorda Ridge anomalies, the Blanco Fracture Zone could deviate from its present orientation only by underthrusting along its length. Peter and Lattimer (1969) imply such underthrusting of the Juan de Fuca sub-plate at the Blanco Fracture Zone when they refer to the destruction of a 250 kilometer section of that plate and compression of the material into the Blanco Fracture Zone. However, the gravity data of Dehlinger et al. (1970) strongly opposes the possibility of such underthrusting. Dehlinger et al. (1970) reported a slightly negative free-air gravity anomaly over the entire Blanco Fracture Zone except in the Blanco trough, where the topography creates a

larger negative anomaly. By contrast, the area of the Mendocino Fracture Zone, where underthrusting is proposed and somewhat substantiated by siesmic refraction studies (Dehlinger et al., 1970) and the first motion earthquake data of Seeber et al. (1970), the gravity data support the idea of consumption of the Gorda sub-plate. The conclusion that there is no subduction along the Blanco Fracture Zone is consistent with the hypothesis presented here.

An additional piece of evidence that the Blanco Fracture Zone has maintained its orientation relative to the boundary plates for at least $2\frac{1}{2}$ million years relates to the formation of the Blanco trough (Melson, 1969), and a corresponding trough in the fracture zone at the northern end of the Gorda Ridge (Figure 26). Because the Blanco Fracture Zone is not perpendicular to the ridges it separates, there is a small area between the edge of the newly formed plate and the fracture zone that is under tension and forms a depression (Sleep et al., 1970; van Andel et al., 1971; Menard and Atwater, 1969). Both troughs are approximately 75 kilometers long. The Blanco trough is 13 kilometers wide (Melson, 1969) and the trough adjacent to the Gorda Ridge is approximately the same width.

Assuming that the tectonic situation is similar to that described for the Vema Fracture Zone (van Andel et al., 1971), the dimensions of the trough provide a means of calculating the age of the trough. Spreading at a rate of 2.9 cm/yr., the ridges could produce a trough

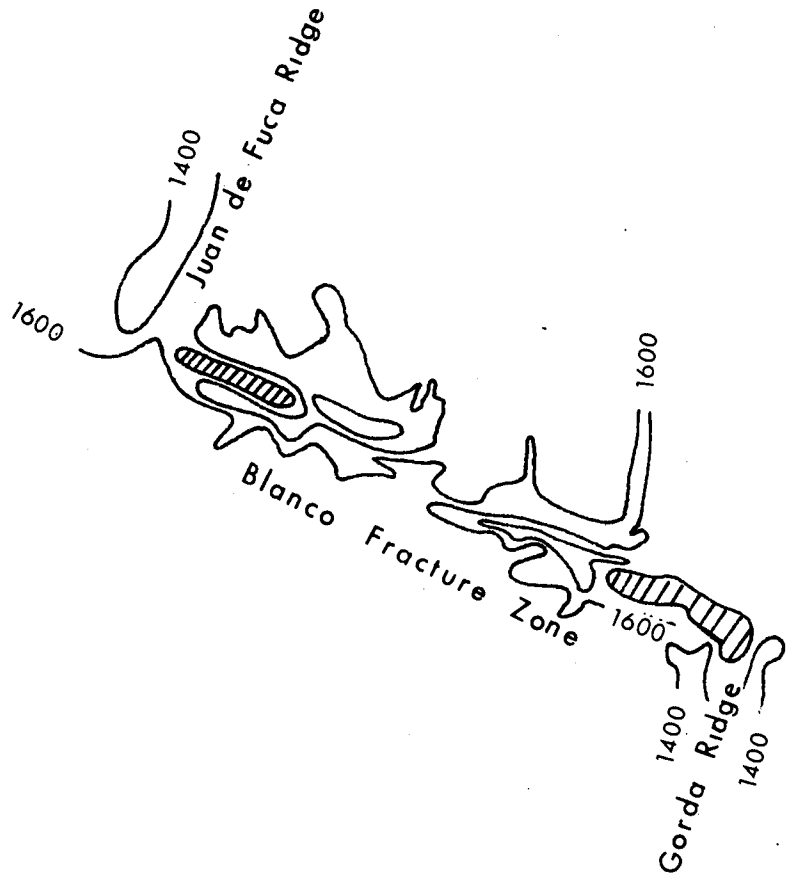

Figure 26. The troughs of the Blanco Fracture Zone are shown in lined pattern.

75 kilometers long in 2.5×10^6 years. Furthermore, the trough should widen at a rate equal to the sine of the angle between the fracture zone and ridge (10°) times the spreading rate of the ridge.

$$\text{Widening rate} = (2.9 \text{ cm/yr}) \ (\text{Sin } 10°)$$

$$= 0.5 \text{ cm/yr}$$

Growing at a rate of 0.5 cm/yr., it would take approximately 2.6×10^6 yr to develop its 13 kilometers of width.

These data are subjective and crude to say the least. They do, however, suggest that the Blanco Fracture Zone has maintained its orientation for at least $2\frac{1}{2}$ million years which is consistent with the proposed reconstruction of the Gorda-Juan de Fuca area.

SUMMARY AND CONCLUSIONS

The magnetic anomalies formed along the Juan de Fuca and Gorda Ridges have grown shorter since anomaly five time. The anomalies on the east side of the Gorda Ridge have been shortened by the overthrusting of the Pacific plate at the Mendocino Fracture Zone, while those on the east side of the Juan de Fuca Ridge have been shortened by left-lateral shear faulting in Cascadia Basin.

A model for the deformation of these two sub-plates, constructed by restoring the magnetic anomalies to their original lengths, allows the development of the sub-plates to be followed since anomaly five time. The changes in spreading direction of the Juan de Fuca

Ridge and the northwest-southeast orientation of the Blanco Fracture Zone developed as responses to the shortening of the Gorda sub-plate. Right-lateral shear faulting in the Cascadia Basin not only shortened the Juan de Fuca sub-plate, but also caused two episodes of rapid subduction of that plate under the Americas plate. The last episode of subduction caused the prominent disconformity in the sediments of Cascadia Basin. It appears that both episodes of shear faulting are also recorded as prominent unconformities in the sediments of the Oregon continental margin.

If the deformation of the Gorda and Juan de Fuca sub-plates are in response to Pacific plate motion, then these plates are not moving with the Pacific plate, and there must be a right-lateral differential motion between them and the Pacific plate. The model suggests that such motion does occur at the ridge crests and it is responsible for the northerly bend in the Pacific plate extension of the Blanco Fracture Zone.

Thus, some of the salient features of magnetic anomaly pattern of the northeastern Pacific Ocean can be attributed to tectonism occurring along with the normal sea floor spreading activity, but not necessarily directly related to it.

BIBLIOGRAPHY

Arrhenius, G. O. S. 1952. Sediment cores from the east Pacific. Reports of the Swedish Deep-Sea Expedition, 1947-1948. 5: 1-227.

Arrhenius, G. O. S. 1963. Pelagic sediments. In: The Sea, M. N. Hill (ed.), Vol. 3. New York, Wiley. p. 655-727.

Atwater, Tanya. 1970. Implications of plate tectonics for the Cenozoic tectonic evolution of western North America. Geol. Soc. Am. Bull. 81:3513-3536.

Atwater, Tanya and H. W. Menard. 1970. Magnetic lineations in the northeast Pacific. Earth and Planet. Sci. Lett. 7:445-450.

Atwater, Tanya and J. D. Mudie. 1968. Block faulting on the Gorda Rise. Sci. 159:729-731.

Barnard, William D., and Dean A. McManus. 1973. Planktonic foraminifera-radiolarian stratigraphy and the Pleistocene-Holocene boundary in the northeast Pacific. Geol. Soc. Am. Bull. 84:2097-2100.

Berger, W. H. 1971. Sedimentation of planktonic foraminifera. Mar. Geol. 11:325-358.

Biscaye, P. E. 1964. Distinction between kaolinite and chlorite in recent sediments by X-ray diffraction. Am. Min. 49:1281-1289.

Biscaye, P. E. 1965. Mineralogy and sedimentation of recent deep-sea clay in the Atlantic Ocean and adjacent seas and oceans. Geol. Soc. Am. Bull. 74:803-832.

Bretz, J. Harlan. 1969. Lake Missoula floods and channeled scabland. J. Geol. 5:503-543.

Bretz, J. H., H. T. V. Smith and G. E. Neff. 1956. Bretz's flood hypothesis. Geol. Soc. Am. Bull. 67:957-1050.

Broecker, Wallace S. 1966. Absolute dating and the astronomical theory of glaciation. Sci. 151:299-304.

Broecker, W. S., D. L. Thurber, J. Goodard, T. Ku, R. K. Matthews, and K. J. Mesolella. 1968. Milankovitch hypothesis supported by precise dating of coral reefs and deep-sea sediments. Sci. 159:297-300.

Campbell, C. D. 1962. Introduction to Washington geology and resources. Washington Department of Conservation, Division of Mines and Geology Information Circular 22-R. Olympia, Washington. 44 p.

Carlson, Paul R. 1968. Marine geology of Astoria Marine Canyon. Ph. D. thesis. Corvallis, Oregon State University. 259 numb. leaves.

Carson, Bobb. 1971. Stratigraphy and depositional history of Quaternary sediments in northern Cascadia Basin and Juan de Fuca Abyssal Plain, northeast Pacific Ocean. Ph. D. thesis. Seattle, University of Washington. 151 numb. leaves.

Carson, Bobb. 1973. Acoustic stratigraphy, structure and history of Quaternary deposition in Cascadia Basin. Deep-Sea Res. 20:387-397.

Chayes, F. 1960. On correlation between variables of constant sum. J. Geophys. Res. 65:4185-4193.

Dauphin, J. P. 1972. Size distribution of chemically extracted quartz used to characterize fine-grained sediments. M. S. thesis. Corvallis, Oregon State University. 63 numb. leaves.

Dehlinger, P. R., R. W. Couch and M. Gemperle. 1967. Gravity and structure of the eastern part of the Mendocino escarpment. J. Geophys. Res. 72:1233-1247.

Dehlinger, Peter, R. W. Couch, D. A. McManus and M. Gemperle. 1970. Northeast Pacific structure. In: The Sea, Arthur Maxwell (ed.), Vol. 4, New York, Wiley. p. 133-190.

Duncan, John R. 1968. Late Pleistocene and post-glacial sedimentation and stratigraphy of deep-sea environments off Oregon. Ph. D. thesis. Corvallis, Oregon State University. 222 numb. leaves.

Duncan, J. R. and L. D. Kulm. 1970. Mineralogy, provenance and dispersal history of late Quaternary deep-sea sands in Cascadia Basin and Blanco Fracture Zone. J. Sed. Pet. 40:874-887.

Duncan, J. R., G. A. Fowler and L. D. Kulm. 1970. Planktonic foraminiferan-radiolarian ratios and Holocene-late Pleistocene deep-sea stratigraphy off Oregon. Geol. Soc. Am. Bull. 81: 561-566.

Duncan, J. R., L. D. Kulm and G. B. Griggs. 1970. Clay mineral composition of late Pleistocene and Holocene sediments of Cascadia Basin, northeastern Pacific Ocean. J. Geol. 78:213-221.

Emilia, D. A. and G. Bodvarsson. 1969. Numerical methods in the direct interpretation of marine magnetic anomalies. Earth and Planet. Sci. Lett. 7:194-200.

Emiliani, C. 1966. Paleotemperature analysis of the Caribbean core P6304-8 and P6304-9 and a generalized temperature curve for the last 425,000 years. J. Geol. 74:106-126.

Ericson, D. B. and G. Wollin. 1968. Pleistocene climates and chronology in deep-sea sediments. Sci. 162:1227-1234.

Ewing, J. and Maurice Ewing. 1967. Sediment distribution on mid-ocean ridges with respect to spreading of the sea floor. Sci. 156:1590-1592.

Ewing, J., M. Ewing, T. Aitken, and W. J. Ludwig. 1968. North Pacific sediment layers measured by seismic profiling. In: The Crust and Upper Mantle of the Pacific Area, Monography 12 of the American Geophysical Union, L. Knopoff, C. L. Drake and J. H. Pembroke (eds.), p. 147-173.

Fowler, G. A. and L. D. Kulm. 1966. A multiple corer. Limn. and Oceanog. 11:630-633.

Fowler, G. A. and L. D. Kulm. 1970. Foraminiferal and sedimentological evidence for uplift of the deep-sea floor, Gorda Rise, northeastern Pacific. J. Mar. Res. 28:321-329.

George, Peter, and Robert Lattimer. 1969. Magnetic structure of the Juan de Fuca-Gorda ridge area. J. Geophys. Res. 74:586-593.

Goldberg, E. D. 1971. Atmospheric dust, the sedimentary cycle and man. Comments on Earth Sciences: Geophysics. 1:117-132.

Griffin, J. J., H. Windom, and E. D. Goldberg. 1968. The distribution of clay minerals in the world ocean. Deep-Sea Res. 15:433-459.

Griggs, G. B. 1969. Cascadia channel: the anatomy of a deep-sea channel. Ph. D. thesis. Corvallis, Oregon State University. 183 numb. leaves.

Griggs, G. B. and L. D. Kulm. 1970. Sedimentation in Cascadia deep-sea channel. Geol. Soc. Am. Bull. 81:1361-1384.

Griggs, G. B., L. D. Kulm, J. R. Duncan, and G. A. Fowler. 1970. Holocene faunal stratigraphy and paleoclimatic implications of deep-sea sediments in Cascadia Basin. Paleogeog., Paleoclim., Paleoeco. 7:5-12.

Griggs, G. B., L. D. Kulm, A. C. Waters and G. A. Fowler. 1970. Deep sea gravel from Cascadia Channel. J. Geol. 78:611-619.

Hamilton, E. L. 1967. Marine geology of abyssal plains in the Gulf of Alaska. J. Geophys. Res. 72:4189-4213.

Hamilton, E. L. and H. W. Menard. 1968. Undistorted turbidites on Juan de Fuca Ridge. (Abst.) Trans. Am. Geophys. Un. 49:208.

Harward, Moyle E. 1970. Unpublished research on preparation of clays for X-ray diffraction. Oregon State University, Department of Soils, Corvallis, Oregon.

Hays, J. D., T. Saito, N. D. Opdyke and L. H. Burckle. 1969. Pliocene-Pleistocene sediments of the equatorial Pacific: their paleomagnetic, biostratigraphic and climatic record. Geol. Soc. Am. Bull. 80:1481-1514.

Heath, G. R. 1968. Mineralogy of Cenozoic deep-sea sediments from the equatorial Pacific Ocean. Ph. D. thesis. San Diego, University of California. 168 numb. leaves.

Heinrichs, D. F. 1970. More bathymetric evidence for block faulting on the Gorda Rise. J. Mar. Res. 28:330-335.

Horn, D. R., M. N. Delach, and B. M. Horn. 1969. Distribution of volcanic ash layers and turbidites in the north Pacific. Geol. Soc. Am. Bull. 80:1715-1724.

Imbrie, John and W. S. Broecker. 1970. Wisconsin climates recorded in Atlantic deep-sea cores. (Abst.) Abstracts with Programs, 1970 Annual Mtgs. of Geol. Soc. America. 2(7):584.

Isacks, Bryant, Jack Oliver and Lynn R. Sykes. 1968. Seismology and the new global tectonics. J. Geophys. Res. 73:5855-5899.

James, N. P., E. W. Mountjoy, and Akio Omura. 1971. An early Wisconsin reef terrace at Barbados, West Indies and its climatic implications. Geol. Soc. Am. Bull. 82:2011-2017.

Kulm, L. D. and J. V. Byrne. 1966. Sedimentary response to hydrography in an Oregon estuary. Mar. Geol. 4:85-118.

Kulm, L. D. and G. A. Fowler. 1971. Shallow structorial elements of the Oregon continental margin within a plate tectonic framework. Abstracts with Programs, 1971 Annual Mtg. Geol. Soc. America. 3(7):628.

Kulm, L. D. and G. A. Fowler. Cenozoic sedimentary framework of the Gorda-Juan de Fuca plate and adjacent continental margin - a review. (in press)

Kulm, L. D., R. von Huene, J. R. Duncan, J. C. Ingle, S. A. Kling, L. M. Musich, D. J. W. Piper, R. M. Pratt, H. Schrader, O. Weser and S. W. Wise. 1973. Initial Reports of the Deep Sea Drilling Project, Vol. XVIII. Washington (U. S. Government Printing Office).

Le Pichon, X. 1968. Sea floor spreading and continental drift. J. Geophys. Res. 73:3661-3697.

Luyendyk, B. P. 1970. Origin and history of abyssal hills in the northeast Pacific Ocean. Geol. Soc. Am. Bull. 81:2237-2260.

McEvilly, T. V. 1968. Seafloor mechanics north of Cape Mendocino, California. Nature 220:901-903.

McManus, D. A., R. E. Burns, C. von der Borch, R. Goll, E. D. Milow, R. K. Olsson, T. Vallier, and O. Weser. 1970. Site 35. In: Initial Reports of the Deep Sea Drilling Project, Vol. 5. Washington (U. S. Government Printing Office) p. 165-202.

Mammerickx, Jacqueline. 1970. Morphology of the Aleutian abyssal plain. Geol. Soc. Am. Bull. 81:3457-3464.

Mason, R. G. and A. D. Raff. 1961. Magnetic survey off the west coast of North America 40 north latitude to 50 north latitude. Geol. Soc. Am. Bull. 72:1267-1270.

Melson, W. G. 1969. Preliminary results of a geophysical study of portions of the Juan de Fuca ridge and Blanco Fracture Zone. ESSA Technical Memorandum C&GSTM -6. U. S. Dept. of Commerce, Environmental Science Services Administration, Coast and Geodetic Survey, Rockville, Maryland. 33 p.

Menard, H. W. 1967. Sea floor spreading, topography and the second layer. Sci. 157:923-924.

Menard, H. W. 1969. The deep-sea floor. Sci. American. 221(3):126-145.

Menard, H. W. and Tanya Atwater. 1968. Changes in direction of sea floor spreading center. Nature. 219:463-467.

Menard, H. W. and Tanya Atwater. 1969. Origin of fracture zone topography. Nature 222:1037-1040.

Moore, G. W. 1970. Sea floor spreading at the junction between the Gorda Rise and Mendocino Ridge. Geol. Soc. Am. Bull. 81:2817-2824.

Morgan, W. Jason. 1968a. Pliocene reconstruction of the Juan de Fuca Ridge. Trans. Am. Geophys. Un. 49:327. (Abst. only)

Morgan, W. Jason. 1968. Rises, trenches, great faults and crustal blocks. J. Geophys. Res. 73:1959-1982.

Nelson, Carlton H. 1968. Marine geology of the Astoria deep-sea fan. Ph. D. thesis. Corvallis, Oregon State University. 287 numb. leaves.

Opdyke, N. D. and J. H. Foster. 1970. Paleomagnetism of cores from the North Pacific. Geol. Soc. Am. Memoir 126:83-119.

Parkin, D. W., D. R. Phillips, R. A. L. Sullivan and L. Johnson. 1970. Airborne dust collections over the north Atlantic. J. Geophys. Res. 75:1782-1793.

Pavoni, N. 1966. Tectonic interpretation of the magnetic anomalies southwest of Vancouver Island. Pure Applied Geophys. 63: 172-196.

Peter, B. and R. Lattimore. 1969. Magnetic structure of the Juan de Fuca-Gorda Ridge area. J. Geophys. Res. 74:586-593.

Peter, G. and Omar DeWald. 1971. Deformation of the sea floor off the northwest coast of the United States. Nat. Phys. Sci. 232:97-98.

Peterson, R. E. 1969. Calcium carbonate, organic carbon and quartz in hemipelagic sediments off Oregon: a preliminary investigation. M. S. thesis. Corvallis, Oregon State University. 44 numb. leaves.

Pitman, Walter C. III and Dennis E. Hayes. 1968. Sea floor spreading in the Gulf of Alaska. J. Geophys. Res. 73:6571-6580.

Rex, R. W. 1970. X-ray mineralogy, Appendix III. In: Bader, R. G. et al. , Initial Reports of the Deep Sea Drilling Project. Vol. 4. Washington (U. S. Government Printing Office) p. 748-753.

Rex, R. W. and E. D. Goldberg. 1958. Quartz content of pelagic sediments of the Pacific Ocean. Tellus. 10(1):153-159.

Rex, R. W. 1958. Quartz in sediments of the central and North Pacific Basin. Ph. D. thesis. San Diego, University of California. 110 numb. leaves.

Rex, R. W. and E. D. Goldberg. 1962. Insolubles. In: The Sea, M. N. Hill (ed.), Vol. 1. New York, Wiley. p. 295-304.

Richmond, G. M., R. Fryxell, G. E. Neff, and P. L. Weis. 1965. The cordilleran ice sheet of the northern Rocky Mountains and related Quaternary history of the Columbia plateau. In: The Quaternary of the United States, H. E. Wright and D. G. Frey (eds.), Princeton, University Press. p. 231-241.

Rieger, Samuel and Henery Smith. 1955. Soils of the Palouse loess: II Development of the A_2 horizon. Soil Sci. 79:301-321.

Ruddiman, W. F. 1971. Pleistocene sedimentation in the equatorial Atlantic: stratigraphy and faunal paleoclimatology. Geol. Soc. Am. Bull. 82:283-302.

Russell, Kenneth L. 1967. Clay mineral origin and distribution on Astoria Fan. M. S. thesis. Corvallis, Oregon State University. 47 numb. leaves.

Seeber, Leonardo, M. Barazangi and A. Nowroozi. 1970. Micro-earthquake seismicity and tectonics of coastal northern California. Bull. Seismolog. Soc. Am. 60:1669-1699.

Shackleton, N. J. and N. D. Opdyke. 1973. Oxygen isotope and paleomagnetic stratigraphy of equatorial Pacific core V28-238: oxygen isotope temperatures and ice volumes on a 10^5 and 10^6 year scale. Quaternary Res. 3:39-55.

Silver, E. A. 1969. Structure of the continental margin off northern California, north of the Gorda escarpment. Ph. D. thesis. San Diego, University of California. 123 numb. leaves.

Silver, E. A. 1971a. Tectonics of the Mendocino triple junction. Geol. Soc. Am. Bull. 82:2965-2978.

Silver, E. A. 1971b. Small plate tectonics in the northwestern Pacific. Geol. Soc. Am. Bull. 82:3491-3496.

Silver, E. A. 1972. Pleistocene tectonic accretion of the continental slope of Washington. Mar. Geol. 13:239-249.

Sleep, N. H. 1969. Sensitivity of heat flow and gravity to mechanism of sea floor spreading. J. Geophys. Res. 74:542-549.

Sleep, N. H. and Shawn Biehler. 1970. Topography and tectonics at intersections of fracture zones with central rifts. J. Geophys. Res. 75:2748-2752.

Spigai, J. J. 1971. Marine geology of the continental shelf off southern Oregon. Ph. D. thesis. Corvallis, Oregon State University. 214 numb. leaves.

Tobin, D. G. and L. R. Sykes. 1968. Seismicity and tectonics of the northeast Pacific Ocean. J. Geophys. Res. 73:3821-3845.

van Andel, Tj. H. and P. D. Komar. 1969. Ponded sediments of the mid-Atlantic ridge between 22° and 23° north latitude. Geol. Soc. Am. Bull. 80:1163-1190.

van Andel, Tj. H., R. P. von Herzen, and J. D. Phillips. 1971. The Vema Fracture Zone and the tectonics of transverse shear zones in oceanic crust. Mar. Geophys. Res. 1:261-283.

Veeh, H. H. and John Chappell. 1970. Astronomical theory of climatic change: support from New Guinea. Sci. 167:862-865.

Vine, J. 1966. Spreading of the ocean floor: new evidence. Sci. 154:1405-15.

Vine, F. J. 1968. Magnetic anomalies associated with mid-ocean ridges. In: The History of the Earth's Crust, Robert Phinney (ed.), Princeton University Press, Princeton, New Jersey. p. 73-83.

von Huene, R. and L. D. Kulm. 1973. Tectonic summary of Leg 18. In: Kulm, L. D., R. von Huene et al., 1973 Initial Reports of the Deep Sea Drilling Project, Volume 18. Washington (U. S. Government Printing Office). p. 961-976.

von Huene, R., L. D. Kulm, J. R. Duncan, J. C. Ingle, S. A. Kling, L. M. Musich, D. J. W. Piper, R. M. Pratt, H. Schrader, O. Weser and S. W. Wise. 1971. Deep Sea Drilling Project, Leg. 18. Geotimes. 16:12-15.

Windom, H. L. 1969. Atmospheric dust records in permanent snowfields: implications to marine sedimentation. Geol. Soc. Am. Bull. 80:761-782.

Wilson, J. T. 1965. Transform faults, oceanic ridges and magnetic anomalies southwest of Vancouver Island. Sci. 150:482-485.

APPENDICES

APPENDIX 1

Results of the Mineral Analyses

Explanation

The clay mineral concentrations, silt mineral concentrations and faunal counts were each summed to 100% so each group's percentages are relevant to the other minerals in that group and not to the amounts in the total sample.

The body of the tables are the percentages. The depths are in centimeters. Asterisk by the depth means that the sample is from the pilot core.

Samples 110-114, 137-139, 151-163 have anomalously low smectite content, apparently due to treatment with citrate-dithonite. These samples were not included in the clay mineral summary.

Cores Used in This Study

Core Number	Location	Water Depth
6808-4	45°09.6'N, 129°50.7'W	2700 m
6808-5	46°04.6'N, 131°00.7'W	2780 m
6808-6	46°25.1'N, 131°40.4'W	3155 m
6808-8	46°42.0'N, 131°01.0'W	2598 m
6908-5	46°39.1'N, 129°08.0'W	2600 m
6910-1	41°13.4'N, 126°22.5'W	3072 m
6910-2	41°15.8'N, 127°01.3'W	2615 m
6910-3	41.17.0'N, 127°21.7'W	2880 m
6910-4	41°18.8'N, 128°09.0'W	3130 m
7004-1	42°32.0'N, 127°37.5'W	2960 m
7004-3	42°01.5'N, 126°18.1'W	3503 m
7004-4	41°41.0'N, 126°18.1'W	3030 m
7004-6	41°40.0'N, 126°28.6'W	2750 m
7004-7	42°19.5'N, 126°15.0'W	2650 m

CORE 6808-4

Location: 45°09.6' N, 129°50.7' W Water depth 2700 m

Sample number	Depth	CLAYS			SILTS				COARSE FRACTION	
		Smectite	Illite	Chlorite	Feldspar	Quartz	Chlorite	Mica	Rads	Forams
1	6	28	36	37	26	50	16	8		
2	34	10	51	38	21	42	20	16		
3	63	28	40	31	20	44	18	18		
4	81	29	33	38	21	53	17	10		
5	155	27	34	38	20	45	20	14		
7	245	44	26	30	20	48	18	13		
8	299	0	28	72	15	47	22	16		
9	375				23	54	15	8		
10	434	17	43	40	22	40	24	14		
12	564	18	48	33	22	39	23	16		
13	624	33	27	40	23	52	18	6		
14	710	7	30	64	21	48	22	9		
15	735									

CORE 6808-5

Location: 46°04.6' N, 131°00.7' W Water depth: 2780 m

Sample number	Depth	CLAYS			SILTS				COARSE FRACTION	
		Smectite	Illite	Chlorite	Feldspar	Quartz	Chlorite	Mica	Rads	Forams
151	14	0	49	51	18	57	19	6	5	95
152	93	10	49	41	16	55	17	11	0	100
153	200	5	50	45	22	45	22	10	0	100
154	300	0	47	53	20	46	24	9	0	100
155	400	12	49	39	26	47	18	9	0	100
156	500	3	54	43	22	54	16	8	0	100
157	600	7	51	42	24	44	20	12	0	100
158	700	13	52	35	23	52	16	8	0	100
159	800	3	53	44	19	55	20	6	0	100
160	900	5	63	32	20	58	13	8	0	100
161	1000	5	60	35	20	56	15	9	0	100
162	1100	10	59	30	19	49	20	12	0	100
163	1200	13	56	32	21	61	12	6	0	100

CORE 6808-6

Location: 46°25.1' N, 131°40.4' W Water depth: 3155 m

Sample number	Depth	Smectite	Illite	Chlorite	Feldspar	Quartz	Chlorite	Mica	Rads	Forams
103	6	14	53	33	21	58	16	5	5	95
104	100	11	55	33	16	50	17	17	0	100
105	200	12	54	33	20	53	17	10	0	100
106	300	17	48	34	21	54	12	12	0	100
107	400	14	54	32	21	53	13	13	0	100
108	500	27	41	31	20	50	17	13	0	100
109	600	23	42	35	22	49	17	11	0	100
110	702	3	54	43	19	44	23	13	0	100
111	800	8	53	39	20	44	23	13	0	100
112	900	8	61	30	21	44	22	12	0	100
113	1000	7	58	35	27	43	18	11	0	100
114	1100	5	51	43	26	47	18	9	0	100

CORE 6808-8

Location: 46°42.0' N, 131°01.0' W Water depth: 2598 m

Sample number	Depth	CLAYS			SILTS				COARSE FRACTION	
		Smectite	Illite	Chlorite	Feldspar	Quartz	Chlorite	Mica	Rads	Forams
137	3	0	54	46	16	55	20	8		
138	100	4	45	51	22	50	16	11		
139	200	0	54	46	22	55	15	8		

CORE 6908-5

Location: 46°39.1' N, 129°08.0' W Water depth: 2600 m

Sample number	Depth	CLAYS			SILTS			
		Smectite	Illite	Chlorite	Feldspar	Quartz	Chlorite	Mica
31	9	31	39	30	22	42	20	16
32	32	35	39	26	19	36	23	22
33	124	36	34	30	24	37	20	17
34	135	33	36	31	15	30	32	23
35	145	25	40	35	20	42	24	14
36	155	34	35	31	21	48	20	11
37	165	34	33	33	19	42	24	15
38	190	32	31	37	21	42	26	11
39	200	30	33	38				
40	210	30	31	38	22	46	21	11
41	220	29	32	39	24	47	20	19
42	350	29	50	20	17	54	12	18
43	365	32	32	36	20	49	20	10
44	380	31	32	37	21	59	14	6

CORE 6908-5, continued

Sample number	Depth	CLAYS			SILTS			
		Smectite	Illite	Chlorite	Feldspar	Quartz	Chlorite	Mica
45	540	38	32	29	18	46	22	14
46	550	27	34	39	21	42	23	14
47	560	27	36	38	24	48	18	9
48	825	18	45	37				
49	845	22	45	33	17	41	24	18

CORE 6910-1

Location: 41°13.4' N, 126°22.5' W Water depth: 3072 m

Sample number	Depth	CLAYS			SILTS				COARSE FRACTION	
		Smectite	Illite	Chlorite	Feldspar	Quartz	Chlorite	Mica	Rads	Forams
245	0*				20	54	21	5		
246	29*				20	55	20	5		
62	10	17	54	28	20	50	23	7	74	26
63	100	13	42	45	18	49	24	9	93	7
64	200	10	48	42	21	51	21	7	63	37
65	300	9	59	33	20	43	23	14	3	97
66	400	6	57	36	19	47	18	15	20	80
194	481				19	53	21	6	50	50
67	500	8	55	37	21	38	24	17	10	90
195	515				17	42	23	17	- Barren -	
68	560	10	47	43	22	52	20	5	31	69
69	600	6	48	45	20	51	23	6	- Barren -	
70	700	6	56	38	19	46	24	10	- Barren -	
71	800	8	55	37	18	44	22	15	19	81
72	900	12	50	39	19	47	21	13	32	68

CORE 6910-2

Location: 41°15.8' N, 127°01.3' W Water depth: 2615 m

Sample number	Depth	CLAYS			SILTS				COARSE FRACTION	
		Smectite	Illite	Chlorite	Feldspar	Quartz	Chlorite	Mica	Rads	Forams
247	0*				17	55	23	5		
249	57*				18	51	24	8		
190	0				19	50	25	6	95	5
50	8	13	46	41	19	48	24	9	85	15
191	25				19	52	24	5	77	23
51	101	14	44	42	21	50	22	7	0	100
52	223	14	47	39	20	50	24	6	5	95
53	300	13	48	38	19	51	22	8	8	92
54	401	12	50	38	20	50	21	8	8	92
55	506	14	47	39	19	47	25	8	5	95
56	601	10	48	42	19	47	25	9	3	97
57	700	9	50	38	20	44	27	9	3	97
212	770								94	6
58	800	12	52	36	20	51	22	7	65	35
213	830								47	53

CORE 6910-2, continued

Sample number	Depth	CLAYS			SILTS				COARSE FRACTION	
		Smectite	Illite	Chlorite	Feldspar	Quartz	Chlorite	Mica	Rads	Forams
59	900	11	44	45	19	51	22	8	3	97
60	1000	11	50	39	18	50	25	7	45	55
61	1036	11	43	46	19	52	21	8	15	85
222	1*								99	1
223	20*								100	0
224	40*								95	5
225	58*								95	5
226	1								99	1
227	20								100	0
228	40								69	31
229	60								34	66
230	80								45	55
231	100								7	93
232	120								88	12
233	140								27	83

CORE 6910-2, continued

Sample number	Depth	CLAYS			SILTS				COARSE FRACTION	
		Smectite	Illite	Chlorite	Feldspar	Quartz	Chlorite	Mica	Rads	Forams
234	160								21	89
235	180								28	82
236	200								49	51

CORE 6910-3

Location: 41°17.0' N, 127°21.7' W Water depth: 2880 m

Sample number	Depth	CLAYS			SILTS				COARSE FRACTION	
		Smectite	Illite	Chlorite	Feldspar	Quartz	Chlorite	Mica	Rads	Forams
250	0*				17	53	22	8		
251	67*				18	53	21	7		
73	10	12	53	35	20	51	22	7	90	10
192	27				19	48	27	7	47	53
214	40								99	1
74	100	14	47	38	17	43	24	15	1	99
215	106								63	37
193	119				16	48	24	11	3	97
216	138								21	79
75	200	17	43	40	18	46	24	12	1	99
76	300	14	50	36	19	45	24	12	73	27
77	338	17	52	31	18	45	25	11	3	97
78	400	14	49	37	19	45	23	12	10	90
79	500	17	48	35	16	45	25	14	5	95
80	600	11	52	37	18	46	26	10	82	18

CORE 6910-3, continued

Sample number	Depth	CLAYS			SILTS				COARSE FRACTION	
		Smectite	Illite	Chlorite	Feldspar	Quartz	Chlorite	Mica	Rads	Forams
81	700	13	52	35	19	43	27	10	0	100
82	800	10	46	44	21	46	24	8	3	97
83	900	9	56	35	18	40	22	19	0	100
84	1000	16	45	39	19	41	26	18	- Barren -	
85	1100	13	48	38	16	38	28	18	65	35
86	1154	11	58	30	13	31	29	27	26	74

CORE 6910-4

Location: 41°18.8'N, 128°09.0' W Water depth: 3130 m

Sample number	Depth	CLAYS			SILTS				COARSE FRACTION	
		Smectite	Illite	Chlorite	Feldspar	Quartz	Chlorite	Mica	Rads	Forams
87	5	9	51	38	19	50	22	8	80	20
88	70	11	50	37	17	46	24	12	62	38
89	200	13	46	40	21	47	23	9	0	100
196	280				19	48	22	10	5	95
90	298	14	52	33	17	43	30	10	0	100
197	318				17	49	25	8	5	95
91	400	13	51	34	16	48	28	8	0	100
92	500	19	43	37	19	44	25	12	4	96
93	600	18	48	32	19	43	24	14	0	100
198	680				18	45	26	10	5	95
94	703	16	45	38	21	48	19	11	61	39
199	745				19	51	21	9	9	81
95	800	27	43	29	17	50	25	8	0	100
204	820				20	50	23	7	60	40
96	900	23	49	26	18	51	24	7	19	81

CORE 6910-4, continued

Sample number	Depth	CLAYS			SILTS				COARSE FRACTION	
		Smectite	Illite	Chlorite	Feldspar	Quartz	Chlorite	Mica	Rads	Forams
97	1000	17	50	32	19	48	23	10	8	92
98	1100	24	42	33	22	44	24	10	0	100
99	1174	14	54	32	20	42	28	10	0	100
100	1300	18	47	33	18	47	25	10	0	100
101	1362	17	55	28	23	44	19	13	- Barren -	
102	1385	21	45	33	18	51	22	9	0	100

CORE 7004-1

Location: 42°32.0' N, 127°37.5' W Water depth: 2960 m

Sample number	Depth	CLAYS			SILTS				COARSE FRACTION	
		Smectite	Illite	Chlorite	Feldspar	Quartz	Chlorite	Mica	Rads	Forams
237	1*				16	50	26	8		
238	29*				18	48	26	7		
140	20	9	44	47	19	50	25	6	91	9
141	100	6	40	53	20	47	25	7	26	74
142	200	8	44	48	17	45	26	11	10	90
143	300	7	43	50	18	48	25	10	30	70
144	400	7	48	44	20	43	29	10	7	93
145	500	7	47	45	20	42	28	9	15	85
202	580				17	45	29	9	9	91
146	600	9	50	40	20	52	21	6	85	15
203	620				19	50	23	8	100	0
147	700	6	48	46	17	45	31	7	21	79
148	800	9	44	46	20	44	25	10	0	100
149	900	7	46	46	20	48	23	9	0	100
150	1018	8	41	47	20	51	23	7	9	91

CORE 7004-3

Location: 42°01.5' N, 126°18.1' W Water depth: 3503 m

Sample number	Depth	CLAYS			SILTS				COARSE FRACTION	
		Smectite	Illite	Chlorite	Feldspar	Quartz	Chlorite	Mica	Rads	Forams
164	30	12	47	41	19	48	26	8	92	8
165	100	13	37	50	18	43	31	8	50	50
166	200	8	43	48	18	47	26	9	45	55
167	300	6	45	49	24	47	21	8	80	20
168	400	6	47	46	20	53	22	5	41	59
169	500	7	46	46	22	50	20	8	50	50
170	600	5	47	48	17	46	25	11	5	95
171	700	6	44	48	24	50	18	8	0	100
172	800	8	44	48	19	49	23	8	21	79

CORE 7004-4

Location: 41°41.0' N, 126°18.1' W Water depth: 3030 m

Sample number	Depth	CLAYS			SILTS				COARSE FRACTION	
		Smectite	Illite	Chlorite	Feldspar	Quartz	Chlorite	Mica	Rads	Forams
241	0*				19	47	26	7		
242	45*				25	51	18	5		
126	0	18	47	35	19	51	25	5	80	20
217	40								100%	0
218	60								74%	26
219	71								64	36
127	100	15	48	36	22	50	20	8	50	50
220	148								36	64
221	223								16	84
209	200								73	27
128	300	15	43	42	22	43	26	9	17	83
129	400	16	46	38	20	49	23	7	12	88
130	500	13	50	37	21	48	23	8	10	90
131	600	15	48	37	18	50	23	9	33	66

CORE 7004-4, continued

Sample number	Depth	CLAYS			SILTS				COARSE FRACTION	
		Smectite	Illite	Chlorite	Feldspar	Quartz	Chlorite	Mica	Rads	Forams
132	700	18	46	36	19	48	23	10	20	80
133	800	17	52	31	21	48	23	7	58	42
134	830	13	49	38	19	50	25	5	39	61
135	900	12	46	41	21	52	22	5	34	66
136	940	15	46	36	21	45	28	6	27	73

CORE 7004-6

Location: 41°40.0' N, 126°28.6' W Water depth: 2750 m

Sample number	Depth	CLAYS			SILTS				COARSE FRACTION	
		Smectite	Illite	Chlorite	Feldspar	Quartz	Chlorite	Mica	Rads	Forams
240	0*				22	51	21	6		
239	49*				18	50	25	7		
115	0	19	41	39	20	46	28	7	85	15
207	30								83	17
208	70								17	83
116	100	25	39	36	20	52	20	9	93	7
117	200	16	41	42	20	47	25	8	15	85
118	300	24	41	35	17	54	22	5	10	90
119	400	16	50	34	21	50	21	8	35	65
120	500	20	40	38	19	49	23	8	22	78
121	600	19	37	44	21	50	23	6	49	51
122	700	16	46	38	20	52	21	7	59	41
123	800	15	50	35	20	53	22	5	100	0
124	900	16	50	34	19	53	23	5	59	41
125	967	15	48	37	21	45	26	8	2	98

CORE 7004-7

Location: 42°19.5' N, 126°15.0' W Water depth: 2650 m

Sample number	Depth	CLAYS			SILTS				COARSE FRACTION	
		Smectite	Illite	Chlorite	Feldspar	Quartz	Chlorite	Mica	Rads	Forams
243	0*				21	50	24	5		
244	39*				20	54	19	6		
173	13	9	42	49	20	49	24	6	100	0
174	100	6	41	53	16	47	29	7	14	86
175	180	6	45	49	22	47	24	7	1	99
176	600	8	45	47	19	47	27	7	32	68
177	700	7	40	52	20	49	25	5	19	81
200	750				17	50	24	9	34	66
178	770	6	41	53	21	43	26	10	47	53
201	790				16	48	27	9	49	51
205	850				18	51	24	7	90	10
179	870	8	47	45	20	52	22	5	0	100
206	890				17	51	26	6	31	69
180	970	6	42	52	21	44	28	6	2	98

CORE 7004-7, continued

Sample number	Depth	CLAYS			SILTS				COARSE FRACTION	
		Smectite	Illite	Chlorite	Feldspar	Quartz	Chlorite	Mica	Rads	Forams
181	1070	4	42	54	21	43	30	7	10	90
211	1131								71	29
210	1151								94	6
182	1158	7	41	51	20	48	28	5	92	8

THERMOPROBE CORES

Locations: see following page

Core number	Sample number	Depth	CLAYS			SILTS			
			Smectite	Illite	Chlorite	Feldspar	Quartz	Chlorite	Mica
T-3	16	11	17	40	43	18	46	28	8
T-4	17	17	19	40	41	21	46	24	9
T-6	18	30	29	36	35	23	47	21	8
T-7	19	2	14	46	39	17	45	27	10
T-7	20	30	19	40	40	20	51	20	9
T-8	21	10	21	44	35	19	50	21	9
T-10	22	12	16	41	42	18	52	22	8
T-11	23	10	17	43	40	21	52	20	6
T-12	24	10	18	42	32	19	50	22	10
T-13	25	10	20	49	31	20	47	24	8
T-14	26	10	10	40	40	20	52	22	6
T-18	27	1	20	40	40	19	50	23	8
T-18	28	40	19	49	32	21	55	18	6
T-24	29	12	16	41	42	15	43	31	11
T-25	30	11	13	46	41	18	43	30	8

Thermoprobe Core Locations

Station	Latitude	Longitude	Water Depth
T-3	42°42.0' N	126°06.0' W	2506 m
T-4	42°53.3' N	126°34.9' W	2875 m
T-6	43°04.9' N	127°19.5' W	2835 m
T-7	42°33.4' N	127°23.2' W	2670 m
T-10	42°10.0' N	126°44.9' W	2740 m
T-11	42°01.0' N	126°30.5' W	3275 m
T-12	41°49.5' N	126°11.0' W	2925 m
T-13	41°40.0' N	126°19.5' W	3000 m
T-14	41°40.0' N	126°38.0' W	2630 m
T-18	41°40.2' N	127°56.8' W	3180 m
T-24	43°04.3' N	125°40.0' W	3015 m
T-25	43°28.0' N	125°21.0' W	2670 m

APPENDIX 2

Size Fractions of Some Selected Samples

Core	Depth	Less than 2 microns	2-10 microns	Greater than 20 microns
6910-4	1200 cm	71.5%	28%	0.5%
6910-3	1000 cm	61%	36%	3%
6910-1	100 cm	62%	36%	2%
6910-1	488 cm	63%	34%	3%
6910-1	400 cm	50%	48%	2%
7004-4	500 cm	58%	39%	3%
7004-4	600 cm	58%	39%	3%

The size fractionation was accomplished using replicate Stokes' settling to remove the entire fraction from the sample, rather than employing the aliquot techniques commonly used. The procedure was identical to that used to separate the size fractions for mineral analysis as described in the text.

APPENDIX 3

Carbon-14 Dates

Core	Depth Interval	Age in years B.P.
6910-1	120-155 cm	10,050 ± 150
6910-2	80-123 cm	14,520 ± 240
6910-2	222-266 cm	29,950 ± 1450

APPENDIX 4

A Compilation of 2 to 20 micron Quartz Sedimentation Rates

Gorda Ridge Sediments

Data	Source
1. 2-20 micron fraction constitutes 37% by weight of total sample	This report
2. 15% of the 2-20 micron fraction is quartz	Dauphin (1972)
3. Thus, 5.5% of total sample is 2-20 micron quartz	This report
4. Total sedimentation rate equals approximately 10 cm/1000 yrs.	This report
5. 2-20 micron sedimentation rate is 3.7 cm/1000 yrs.	This report
6. 2-20 micron quartz sedimentation rate is .55 cm/1000 yrs.	

Snowfield Studies

1. Eolian sedimentation rate is .21 mm/1000 yrs.	Windom (1969) Mt. Olympus sample
2. 42% is between 2 and 30* microns	Windom (1969)
3. 26% of this size fraction is quartz	Windom (1969) Thesis data

*Windom uses a 30 micron upper limit while this report uses a 20 micron upper limit. The two figures are roughly comparable, however, because the median eolian silt size is 2 to 10 microns (Rex and Goldberg, 1962).

Appendix 4, continued.

Snowfield Studies (continued)

Then, the approximate 2-20 micron quartz rate is (42%) (26%) (.21 mm/1000 yrs) = .02 mm/1000 yrs.

Deep-Sea Sediments from Central Pacific Away from Turbidite Influence

Data	Source
1. Sedimentation rate varies from 3 to 12 mm/1000 yrs. (I use an arbitrary 4 mm/1000 yrs non-biogenous component)	Opdyke & Foster (1970)
2. 50% of sediments are less than 2 microns in size	Griffin et al. (1968)
3. Assume the other 50% is 2-20 micron	
4. Assume this is 26% quartz	Windom (1969)

Thus, 2 mm/100 yrs is the sedimentation rate of the 2-20 micron fraction and the rate for quartz in this size fraction is .52 mm/1000 yrs.

Atmospheric Dust Studies

1. Dust load of Pacific westerlies is 0.4 to 15 $\mu g/m^3$	Goldberg (1971)
2. Assume that this is 42% 2-30 micron as it is on Mount Olympus	Windom (1969)

Appendix 4, continued.

Atmospheric Dust Studies (continued)

Data	Source
3. Assume that the 20-30 micron fraction is 26% quartz	Windom (1969)
4. Assume uniform dust load up to 5000 meters and that there is a rain-out every week and that the density of the sediment in water is .5 g/cm^3	Ferguson et al. (1969)

Then a maximum quartz sedimentation rate can be computed

$$\frac{(15\ \mu g/m^3)\ (5000\ m^3)\ (50\ wks/yr)\ (1000\ yr)\ (42\%)\ (26\%)}{(10^4\ \frac{cm^2}{m^2})\quad (10^6\ \frac{\mu g}{g})\quad (.5\ g/cm^3)}$$

as .82 mm/1000 yrs.

Rex (1958, page 65) suggests possible sedimentation rates for total dust in the range of 0.1 to 1.0 cm/1000 yrs on the basis of Japanese radioactive dust studies. Assuming that this is 42% 2-20 micron and 26% of this fraction is quartz then one can obtain a maximum possible quartz sedimentation rate of

$$(1.0\ cm/1000\ yrs)\ (42\%)\ (26\%) = .109\ cm/1000\ yrs$$

or 1.1 mm/1000 yrs

Appendix 4, continued.

Summary

Area	2-20 Micron Quartz Sedimentation Rate
Gorda Ridge	5.5/1000 yrs
Snowfield (Mt. Olympus)	.02 mm/1000 yrs
Deep-sea Sediments (North Pacific)	.52 mm/1000 yrs
Atmospheric Dust Studies Westerlies	
Goldberg	.82 mm/1000 yrs
Rex	1.1 mm/1000 yrs

The large number of assumptions and the indiscriminate mixing of data from several workers make any conclusions about the 2-20 micron quartz sedimentation rate very questionable. These data do, however, suggest that as much as 0.4% to 20% of the quartz in the Gorda Ridge sediments could be eolian. However, the figure is probably closer to the low end of the range rather than the high end.